Integration of Multi-Omic Datasets to Associate Plaque Characteristics with DNA methylation (CpGs)

Astrid Hofman
Prof. Dr. Ir. Hester den Ruijter, PhD
September 16th, 2022

Abstract

Objective: Multi-omics datasets were integrated to create a workflow to investigate the association of DNA methylation to plaque biology.

Methods & Results: DNA methylation (n = 492), bulkRNA (n = 654), and single-cell sequencing (n = 46) datasets from carotid plaques obtained through carotid endarterectomy from the AtheroExpress biobank were used. From this, we determined that a CpG site shown to be causal to coronary heart disease, cg26470101, demonstrates increased methylation in fibrous plaques to atheromatous plaques. This association is also independent of sex, while also demonstrating increased methylation in women. Furthermore, using a differential gene expression analysis for cg26470101 methylation levels in bulkRNA sequencing data, it was possible to identify 37 differentially expressed genes (DEGs) linked to cg26470101. These DEGs were then linked to various biological pathways, gene ontologies, and diseases, as well as their expression in smooth muscle cells scRNA sequencing data. Furthermore, it was then found that 59% of the DEGs identified are more expressed in a fibro-cellular plaque phenotype identified in bulkRNA sequencing data.

Conclusion: This research set-up a framework that can be used to link CpG site(s) to plaque biology and eventually enable a more comprehensive understanding of atherosclerotic processes.

Plain-Text Summary

Coronary heart disease is a major cause of death worldwide and can be caused by a disease called atherosclerosis. Atherosclerosis is a chronic condition caused by a buildup of 'plaque' inside your arteries. The coronary arteries are responsible for distributing oxygen-rich blood throughout the body, which is critical for the body to function properly. Without this oxygen-rich blood, vital organs such as your heart do not receive enough oxygen and cannot function properly. The plaques that characterize atherosclerosis are a build-up of fatty substances such as cholesterol and continue to grow over time.

While the exact cause of atherosclerosis is multifactorial, patients with the disease have a build-up of cholesterol in their arteries, which is caused by many factors including but not limited to high blood pressure, age, diabetes, smoking, obesity, and poor diet. Additionally, it is now known that the way atherosclerosis manifests are different between men and women, for instance in how their plaques differ. This makes it especially important to understand what is at the root of these differences. One of these changes that is thought to contribute to these differences is a process called 'DNA methylation'.

DNA is a molecule in the human body that provides the genetic blueprint for how we develop, live and reproduce. It consists of four bases: cytosine, guanine, adenine, and thymine. In some situations, a chemical group called a 'methyl group' is added to the cytosine base, and after this process occurs the DNA is considered methylated. Depending on where on the gene the cytosine that is being methylated is located, the way that a gene is 'read' by the genetic machinery is altered. In the case of DNA methylation, this means the gene is often not read, and therefore it cannot exert its effect. The easiest case to imagine is in the case of cancer: if a cancer-causing gene is methylated, this gene will not be read, and will not be able to cause cancer.

Recently, research has showed that atherosclerotic plaques can also have sites that are methylated, called CpG sites. We hypothesized that DNA methylation is linked to plaque characteristics. However, it is difficult to understand the relationships between DNA methylation and plaque characteristics, so multiple datasets are necessary to put the pieces together. There are datasets with plaque methylation information, which genes are expressed in certain conditions, and a dataset where you can observe in which cells these genes are being read (or not read).

This research wanted to combine information from all these datasets to allow for a more comprehsive understanding of which DNA methylation patterns are related to certain plaque types. To do so, we found that a particular methylation site, that was previously identified to 'cause' coronary heart disease, is methylated more in patients with stable plaques. Furthermore, it is also methylated more in women. This was then linked to several genes that are read at an increased amount at that site, and it was found that these genes are present mostly in smooth muscle cells, a type of cell that is prevalent in stable plaques.

1 Introduction

Coronary heart disease (CHD) is a leading cause of global mortality, which is often caused by atherosclerosis, and is responsible for a myriad of secondary (cardiovascular) events, including but not limited to myocardial infarction (MI), stroke, and transient ischemic attack (TIA).[1] Atherosclerosis is a chornic condition characterized by the accumulation of fatty material and inflammatory components in the intima of the arteries, thereby forming fibrofatty lesions.[2,3] Over time, these fibrofatty lesions progress into atherosclerotic plaques through outward expansion into the arterial wall, which interrupts blood flow and leads to tissue ischemia.[2,4]

Post-mortem histological studies have revealed that atherosclerotic plaques have specific characteristics, which confer to two overarching plaque phenotypes known as the 'vulnerable' plaque and the 'stable' plaque.[5] Vulnerable plaques, also referred to as atheromatous plaques, are composed of a lipid-rich core, a thin fibrous cap, abundant inflammatory cells, and are characterized by intraplaque haemorrhage (IPH).[5,6] Atheromatous plaques have conventionally been viewed as high-risk due to their high likelihood of causing local thrombosis via rupture of the thin fibrous cap, thereby exposing the lipid content of the plaque to the bloodstream.[5] Conversely, stable plaques, also known as fibrous plaques, are characterized by a thick fibrous cap, increased collagen, and higher SMC content.[5,7] Rather than rupturing, fibrous plaques occlude the artery, thereby restricting blood flow to the heart, brain, or lower extremities.[8] While the traditional perspective on plaque phenotype has been according to this binary system, recent transcriptomic-based research indicates the existence of 'intermediate' phenotypes that exhibit different traits.[9]

Various histological, pathological, and clinical studies have found that the clinical burden of atherosclerosis and the plaque composition is related to the sex of a patient.[10–12] Histological analysis of carotid plaques in women have consistently found a higher prevalence of stable plaques [with less inflammation], hinting towards plaque erosion being a more dominant process in women compared to men, independent of cardiovascular risk profile.[7] Men present with more rupture-prone plaques and carry a higher plaque burden and size at younger ages compared to women, and therefore present more frequently with acute clinical events.[13] However, while recent years have brought the concept of sex as a significant biological variable into consideration, much remains unknown about the underlying biological processes that mediate the sex-specific effect on plaque phenotype and clinical outcomes.

Due to the complexity of the processes underlying atherosclerotic plaque formation, many nuanced mechanisms remain elusive. Recent research, however, has implicated a growing role for epigenetics in the development of atherosclerosis.[14] Abnormalities in DNA methylation, the epigenetic process by which a methyl group is added to the C5 position of cytosine residues when followed by guanine, has been linked to development of atherosclerosis.[14,15] This process is partially heritable, but also a process governed by environmental stimuli.[14] Large-scale population studies have found that well-established cardiovascular risk factors including but not limited to smoking, obesity, hypertension, and type 2 diabetes have been implicated in changes in blood leukocyte DNA methylation.[16] This implicates both the global genomic methylation status and methylation at specific loci in atherosclerosis development.[14] However, research studying the effect of DNA methylation on atherosclerosis often focuses on DNA methylation in patient blood, rather than atherosclerotic plaques, despite growing evidence that plaque DNA methylation is associated to atherosclerotic plaque phenotypes.[17]

Recently, a longitudinal study including 11,461 patients studying the epigenome-wide effects of incident CHD events found that 52 CHD-associated CpGs were identified in blood leukocyte levels.[16] For

2 of the 52 CHD-associated CpGs, the authors provided evidence that these CpGs not only linked to CHD risk, but appeared to be causal in its pathophysiology.[16] However, the exact biological mechanism behind this causality was not touched upon. The results of this research found that there is no association between blood and plaque methylation of the CpGs, and therefore we hypothesize that, as atherosclerosis is the main cause of CHD, the same CpGs found to be causal in blood might influence plaque biology through an independent mechanism. Therefore, this research aimed to determine whether through the integration of multi-omic datasets, it is possible to associate plaque biological characteristics important for atherosclerosis pathophysiology with DNA methylation (CpGs).

2 Results

To establish an association between DNA methylation and plaque characteristics, plaque DNA methylation data from patients undergoing carotid endarterectomy included in the AtheroExpress Biobank study was used (Table 1).

Table 1. Patient Characteristics of patient's whose DNA methylation was measured in the AtheroExpress Biobank Study. Abbreviations: IQR: Inter-quartile range; LDL: low-density lipoprotein; HDL: high-density lipoprotein; eGFR: estimated glomerular filtration rate; CAD: coronary artery disease ; CI: coronary intervention ; TIA: transient ischemic attack ; UMC: university medical center

	Female	Male	P-value
Number of Patients	148	344	
Age (median [IQR])	69.00 [62.00, 74.00]	69.00 [61.00, 74.00]	0.717
Systolic Blood Pressure (median [IQR])	155.00 [140.00, 170.00]	155.00 [135.00, 170.00]	0.297
Diastolic Blood Pressure (median [IQR])	80.00 [75.00, 90.00]	80.00 [73.50, 90.00]	0.971
Hypertension (%)	115 (78.8)	247 (74.4)	0.363
Total Cholesterol (median [IQR])	5.24 [4.06, 5.94]	4.43 [3.60, 5.29]	<0.001
LDL Levels (median [IQR])	3.19 [2.38, 3.81]	2.60 [2.02, 3.30]	0.002
HDL Levels (median [IQR])	1.21 [0.94, 1.51]	1.07 [0.86, 1.28]	0.001
Triglycerides (median [IQR])	1.50 [1.15, 2.06]	1.51 [1.10, 2.04]	0.945
eGFR (median [IQR])	68.45 [54.86, 85.15]	74.02 [60.67, 85.64]	0.050
Smoker (%)	53 (37.1)	90 (26.4)	0.025
History of CAD (%)	42 (28.6)	137 (39.8)	0.023
History of CI (%)	24 (16.3)	95 (27.6)	0.011
History of TIA or Stroke (%)	119 (80.4)	288 (83.7)	0.446
Contralateral Stensosis (%)			0.002
0 - 50%	78 (55.7)	171 (53.4)	
50 - 70%	28 (20.0)	30 (9.4)	
70- 99%	17 (12.1)	47 (14.7)	
100%	17 (12.1)	72 (22.5)	
Ipsilateral Stenosis (%)			0.798
0 - 50%	0 (0.0)	1 (0.3)	
50- 70%	8 (5.6)	20 (6.0)	
70 - 99%	135 (94.4)	315 (93.8)	
Medication Use (%)			
Hypertensive Drugs	108 (73.0)	276 (80.2)	0.096
Antiplatelet Drugs	135 (91.2)	308 (89.5)	0.684
Statins	112 (75.7)	261 (75.9)	1.000
Anticoagulants	16 (10.8)	46 (13.4)	0.524
Symptoms (%)			0.879
Asymptomatic	24 (16.3)	56 (16.3)	
Ocular	22 (15.0)	43 (12.5)	
TIA	65 (44.2)	153 (44.5)	
Stroke	36 (24.5)	92 (26.7)	
Hospital (%)			0.056
UMC Utrecht	97 (65.5)	192 (55.8)	
St. Antonius Nieuwegein	51 (34.5)	152 (44.2)	

2.1 No Correlation between Blood & Plaque Methylation Levels

The two CpGs identified as causal for CHD in blood leukocyte levels, cg26470101 and cg07289306, were used as the starting point of this research.[16] To first determine whether the two CpGs act through independent mechanisms in blood and plaque, their respective methylation values were correlated against each other per patient (Figures 1A, 1B ; n = 88). Since there is no strong correlation between the blood and plaque methylation levels for either CpG, we hypothesize that the CpGs act through independent mechanisms in blood and plaque.

To determine how these CpGs present in plaques between patients, the methylation values for cg26470101 and cg07289306 were presented in density plots, respectively (Figures 2C, 2D ; n = 492). This demonstrates a range of variation from 0.17 to 0.48 for cg26470101 and a range of 0.22 to 0.59 for cg07839457. Due to this inter-patient variability, it became of interest to explore the driving force behind this variability.

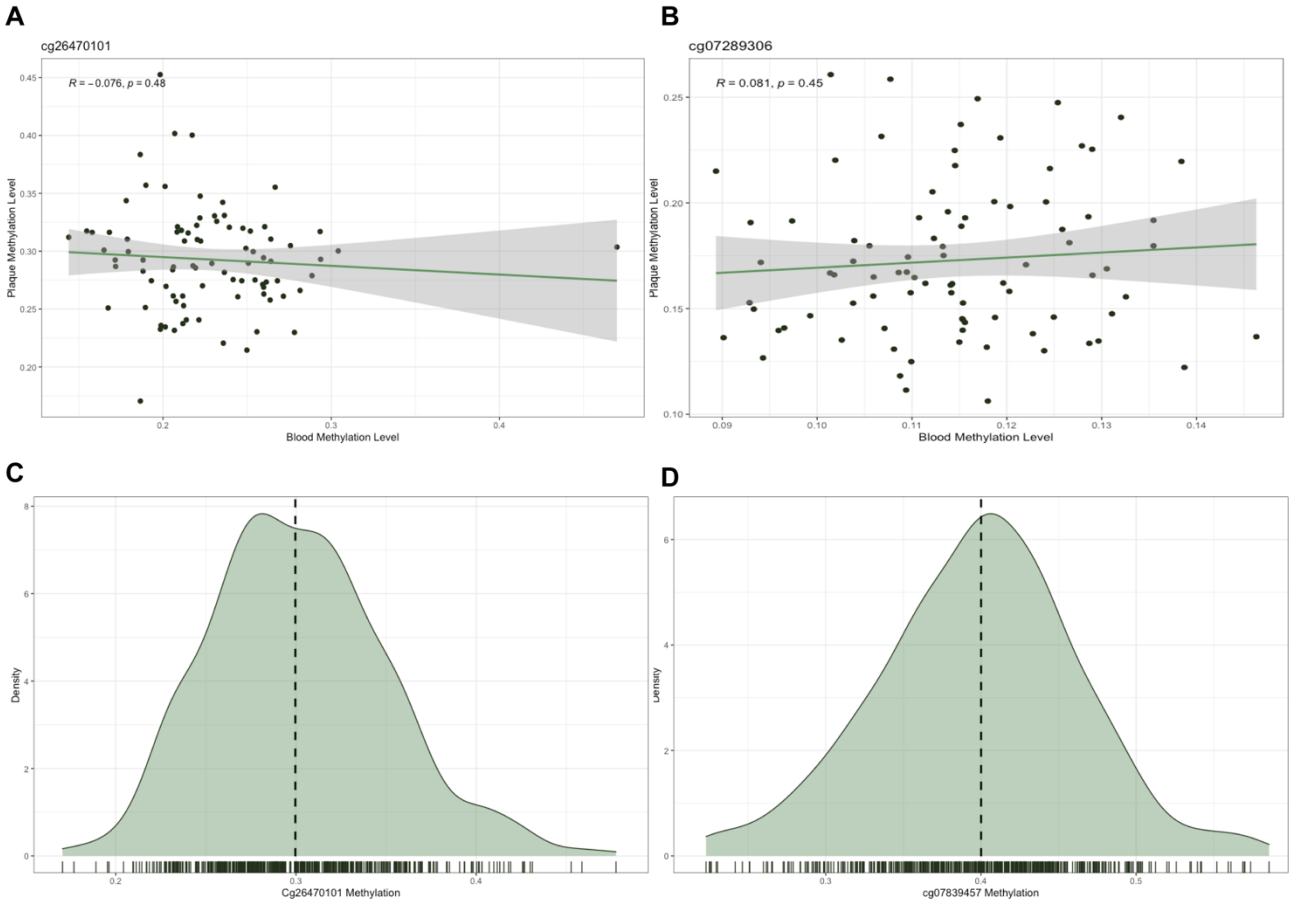

Figure 1. A. Scatter plot showing the blood and plaque methylation levels per patient for cg26470101 (n = 88). B. Scatter plot showing the blood and plaque methylation levels per patient for cg07289306 (n = 88). C. Density plot showing variance in cg26470101 methylation levels (n = 492). D. Density plot showing variance in cg07839457 methylation levels (n = 492).

2.2 Increased cg26470101 methylation levels are associated to a Fibrous Plaque Phenotype and Female Patients

Subsequently, the relationship between the variation in the methylation levels of the CpG and plaque biology was evaluated. Plaque biology relies on cell-type composition, which is captured by the overarching plaque phenotypes: fibrous, atheromatous, and fibroatheromatous (n = 492). To study the potential association of the CPG methylation levels with plaque phenotype, we constructed a linear model where methylation level was used as a continuous dependent variable and plaque phenotype was used as a categorical independent variable with atheromatous plaques as the reference group. There was a significant difference between fibrous and atheromatous plaques, and trend analysis revealed that fibrous plaques show higher cg26470101 methylation ($p = 0.0053$, Figure 2A). Since fibrous plaques are more prevalent in females compared to males, the linear model was adjusted for sex to determine whether the association of cg26470101 with plaque phenotype was independent of sex, which is the case ($p = 0.014$). Additionally, independent of plaque phenotype, females present with higher cg26470101 methylation levels (Figure 2B). As there is no association between plaque phenotype and cg0783957 ($p = 0.578$), only cg26470101 was considered associated with plaque phenotype and included in downstream analysis.

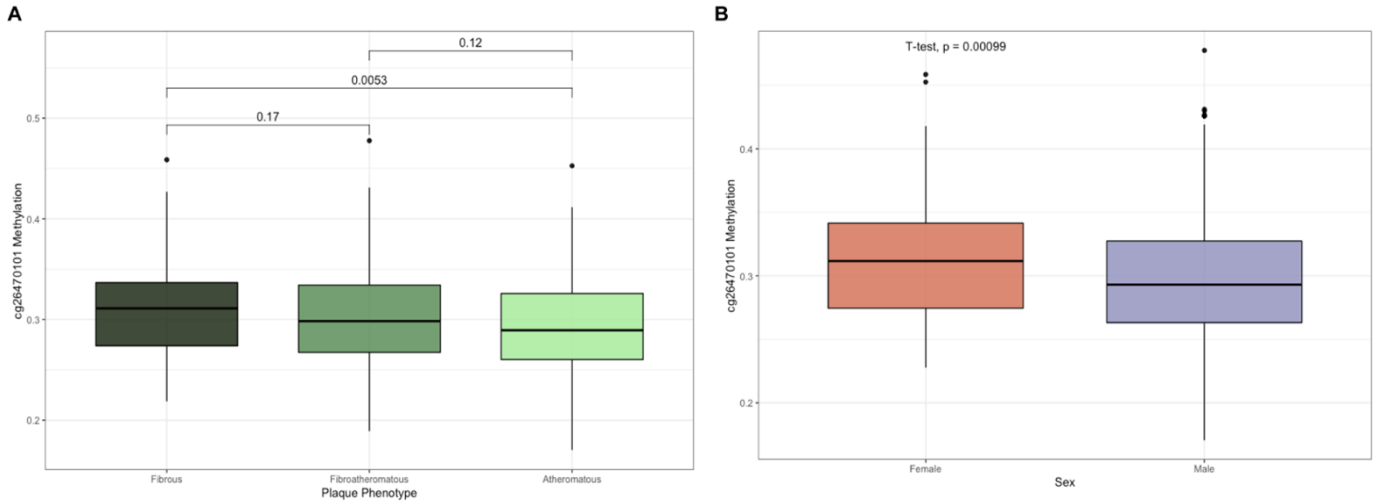

Figure 2. A. Boxplot showing the differences in methylation level for cg26470101 between fibrous, fibroatheromatous, and atheromatous plaques (n = 492). B. Association of cg26470101 methylation between males and females, demonstrating increased methylation in female patients. (n = 492).

2.3 Using Plaque Bulk RNA Sequencing Data to Link Gene Expression to cg26470101 Methylation Levels

It has been established through various GWAS studies that genetic loci are implicated in atherosclerosis, and specifically that lesion composition including fibrous cap thickness, lesion size, and cellular composition are regulated by genetic contributions.[18] Since DNA methylation is known to regulate gene expression, cg26470101 was associated with gene expression levels in plaque bulk RNA sequencing data, to support the findings in plaque DNA methylation data.

2.3.1 *DLX2* and *ITGA6* Expression Show No Correlation to Cg26470101 Methylation

For the CpG sites correlating to CHD risk, Agha et al. used the Illumina annotations (February 2009 – CRCh37/hg19) assembly to determine the gene that the CpG is on or the nearest gene.[16] From this analysis, they concluded that DLX2 is the nearest mapped gene for cg26470101, and from a Mendalian randomization analysis, they found that 84 out of 261 detected methylation quantitative trait loci (meQTL) overlapped with an expression quantitative trait loci (eQTL) for *ITGA6*.[16] When the

expression of *DLX2* was correlated against cg26470101 methylation, there is no correlation between cg26470101 methylation and expression (Figure 3A). Additionally, when the expression of *ITGA6* was correlated against the methylation level of cg26470101, showing that there is no correlation between gene's expression and the methylation of cg26470101 in plaque, further supporting the independent mechanism hypothesis for *ITGA6* (Figure 3B).

2.3.2 Differential Gene Expression (DEG) Analysis Associates 37 Genes with Cg26470101 Methylation

As we hypothesize that cg26470101 may act through a different mechanism in plaque compared to blood, a CpG-specific gene expression analysis was performed, where gene expression was used as a continuous dependent variable and cg26470101 methylation level was used as a continuous independent variable ($Gene_i \sim cg26470101$). Given the association found between cg26470101 and plaque phenotype and the fact that plaque phenotype and gene expression are closely linked, the model was adjusted *a priori* for plaque phenotype to unravel associations of the methylation levels with gene expression independent of plaque phenotype. DEGs with a log2FC greater than or equal to 0.5 and a p-values less than or equal to 10e-5 were visualized in a volcano plot (Figure 3C). 37 genes were significantly associated with cg26470101 independent of plaque phenotype after adjustment for multiple testing. The complete list of genes can be found in Table S1.

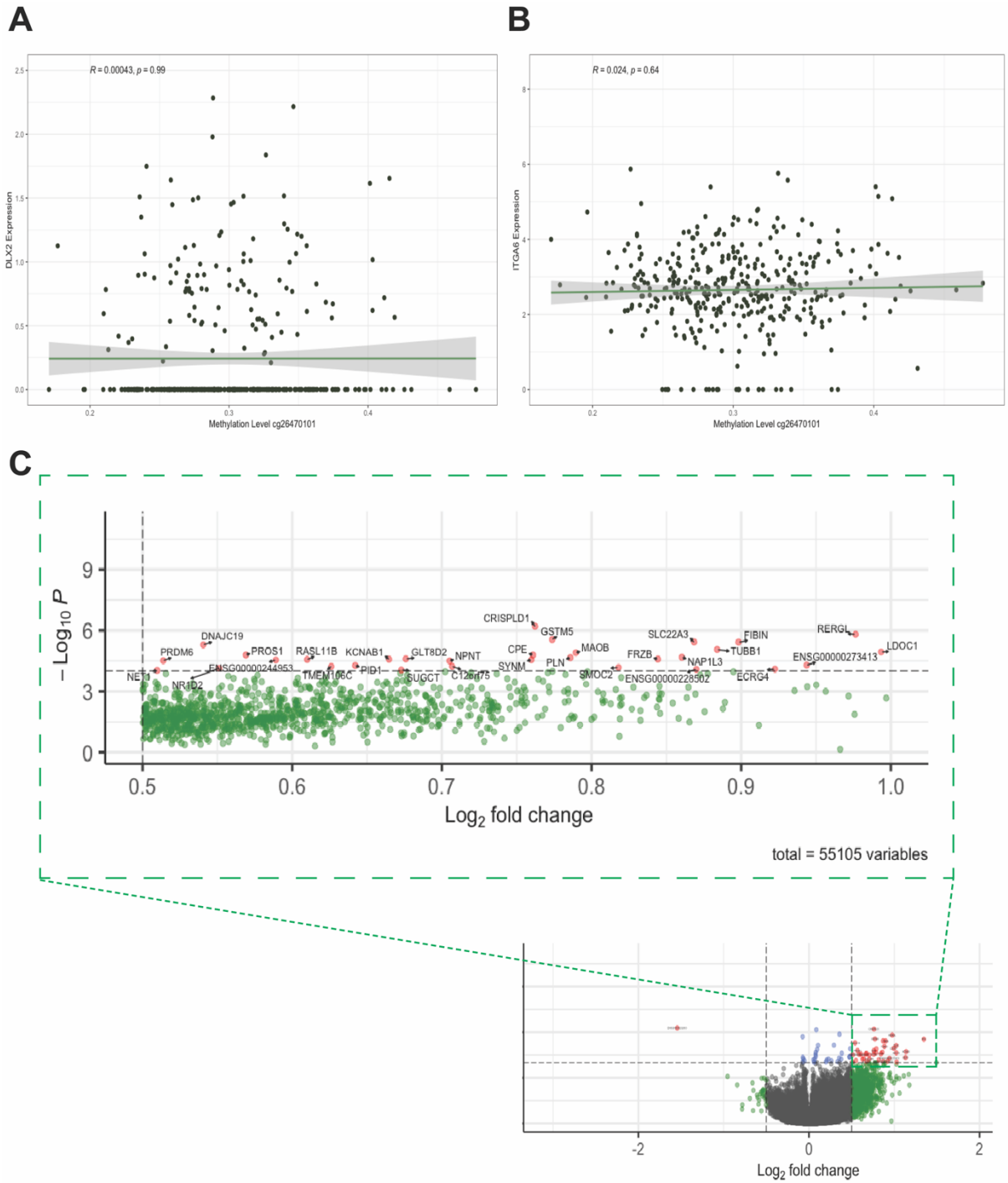

Figure 3. A. Scatter plot showing cg26470101 methylation compared to the expression of DLX2 B. Scatter plot showing cg26470101 methylation compared to ITGA6 expression. C. Volcano plot showing the differential gene expression analysis for cg26470101 using the EnhancedVolcano package.

To then determine whether these genes could be placed into the context of atherosclerosis, Enrichr, an online pathway analysis tool was used to determine which pathways, the ontology, and diseases the 37 DEGs are present or involved in.[19] The complete results can be found in Tables S2-4. Regarding pathways involved, several databases were consulted: Reactome 2016, MSigDB Hallmark, KEGG 2021, and Wikipathways 2021. The Reactome 2016 database reports that several pathways are significant, but notably the common pathway of fibrin clot formation and Abacavir transmembrane transport. The MSigDB Hallmark database also found coagulation and bile acid metabolism. KEGG 2021 (human) found that ABC transporters, cocaine addiction, phenylalanine metabolism, amphetamine addiction,

and more are seemingly linked to the DEGs. Lastly, the Wikipathway 2021 reports involvement of dopamine metabolism, epinephrine and norepinephrine targeted receptors and platelet-mediated interactions with vascular and circulating cells.

For gene ontology, the GO Biological Process 2021 and GO Molecular Function 2021 databases were consulted. Some processes identified include serotonin transport, atrial cardiac muscle cell membrane repolarization, positive regulation of fibroblast growth factor receptor signalling pathway, and cell-cell adhesion mediated by integrin. GO Molecular Function 2021 showed involvement of ATPase inhibitor activity, CXCR3 chemokine receptor binding, all-trans retinal binding, and retinal binding, amongst others (Table S3). Lastly, the GWAS catalog 2019 was used to establish any connection to diseases or drugs. This found involvement of neuritic plaques or neurofibrillary tangles, or cerebral amyloid angiopathy), aging traits and cardiac structure and function, amongst others (Table S4).

2.4 Cg26470101 Methylation, Differentially Expressed Genes & Transcriptomic Clusters

While the traditional perspective on plaque phenotype is based on macroscopic plaque composition assessed through visual inspection, recent research based on gene expression analysis has found that there appear to be different phenotypes, in the form of 5 clusters, that more accurately describe the diversity of plaque phenotypes.[9] These clusters are defined as follows: #0: fibro-collagenous, #1: intermediate, #2: lipomatous, #3: fibro-inflammatory, and #4: fibro-cellular.[9] Since cg26470101 methylation is associated with a fibrous plaque phenotype, it can be hypothesized that cg26470101 methylation associates with clusters enriched for fibrous plaques.

2.4.1 Cg26470101 Methylation Does Not Associate with a Specific Transcriptomic Cluster

To a achieve this, a linear model was constructed, using the CpG as the continuous dependent variable and the transcriptomic clusters as a categorical independent variable (n = 391). As shown in Figure 4A, cg26470101 methylation shows no significant differences between the 5 clusters, and thus the clusters cannot be used to link plaque DNA methylation levels to the transcriptomic clusters.

2.4.2 DEGs Identified Using Bulk RNA Sequencing Data Show Increased Expression in Cluster #4

As the clusters cannot be used to associate cg26470101 methylation with a specific cluster, the DEGs identified in the bulkRNA may show cluster-specific expression. For the 37 DEGs identified from the bulkRNA, 22 (59%) showed increased expression in cluster #4, 12 (32%) in cluster #3, 1 (<1%) in cluster #0, 1 (<1%) equally in clusters #3 and #4, and 1 is not expressed in any of the clusters. 9 randomly selected genes from the 37 DEGs and their expression in each cluster is shown (Figure 4b, Supplemental Figure 1).

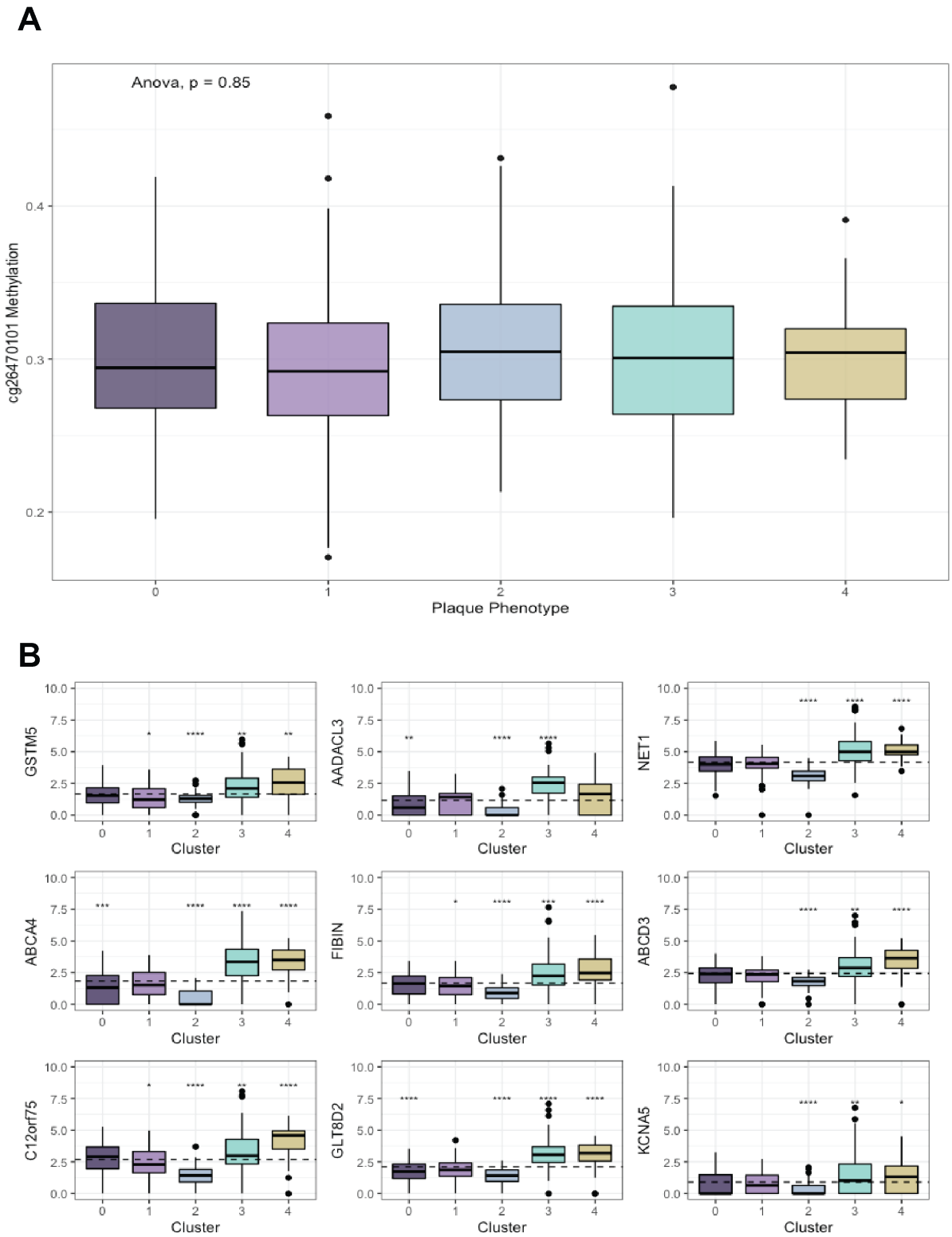

Figure 4. A. Boxplot showing cg26470101 methylation levels for each of the 5 transcriptomic clusters identified to describe atherosclerotic lesions. B. Boxplots showing 9 randomly selected differentially expressed genes and their expression across the 5 transcriptomic clusters.

2.5 Single-Cell Sequencing Data Links DEGs with Smooth Muscle Cell-Specific Expression

Next, the expression of the previously DEGs was explored in single-cell RNA data, to assess cell type-specific expression within the plaque. To assess this, the expression of the 37 genes was displayed in a violin plot (Figure 5). This demonstrates that the strongest cell-type specific expression is in *ACTA2+* SMCs.

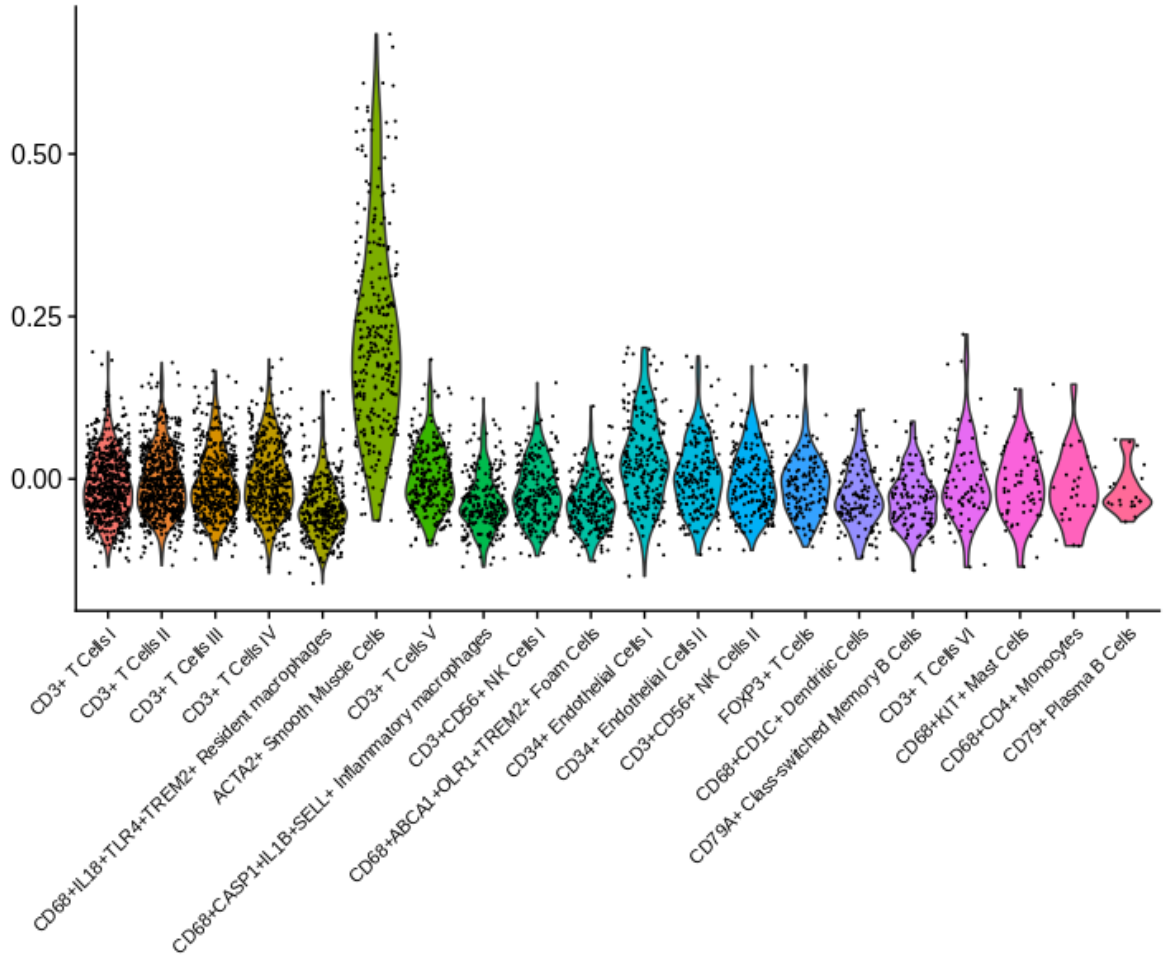

Figure 5. Violin Plot showing the expression of the 37 genes identified via DEG analysis and their expression across different cell types. X-axis showing the cell types present in the single-cell RNA sequencing dataset and the y-axis showing the level of expression.

3 Discussion

3.1 Biological Interpretation of Results

This research aimed to integrate multi-omic datasets to associate DNA methylation in atherosclerosis with plaque biology. To do so, two CpGs identified previously as being causal to CHD in blood leukocyte levels were used as the starting point for this research.[16] It was first determined that there is no correlation between blood and plaque methylation levels for either cg26470101 and cg07839457, which led to the hypothesis that blood and plaque methylation act through different axes. This was further confirmed when the bulkRNA data revealed that there is no correlation between *ITGA6* expression and cg26470101 methylation, two genes known to be associated with cg2647010 in blood. It was also determined that there was a relatively large inter-patient variability in methylation levels of the CpGs, leading to the hypothesis that plaque biology could be driving this variability. This showed that cg26470101 methylation is increased in fibrous plaques and women.

Subsequently, the bulkRNA sequencing data was used to identify 37 DEGs independent of plaque phenotype, which corresponded to various biological processes, pathways or gene ontologies. As expected, some can be easily linked to plaque or vascular biology, whereas other processes seem to have no clear link. For instance, the fibrin clot formation pathway, coagulation, ABC transport, fibroblast growth factor receptor signalling pathway, and platelet mediated actions with circulating and vascular cells have been implicated in CAD.[20–24] However, other processes such as cocaine and amphetamine addiction, dopamine metabolism, and (nor)epinephrine receptors are not directly implicated in the progression of atherosclerotic lesions at time of writing. Therefore, it stands to reason that results from the gene enrichment analysis could serve to validate results, but results should be evaluated thoroughly before deriving meaning from them.

These genes were then linked to transcriptomic clusters, where this revealed that 59% of the DEGs demonstrate increased expression in cluster #4. Cluster #4 is significantly enriched in fibrous plaque with lower fat content and increased numbers of *ACTA2*+ SMCs.[9] This correlates to the results from the scRNA sequencing data, which found that the 37 DEGs are primarily expression in *ACTA2*+ SMCs. This implies that the transition between DEGs and scRNA sequencing data can demonstrate not only which genes are upregulated, but that it can also be easily determined which cell-type is likely contributing to this upregulation. Additionally, it is known that fibrous plaques are composed of increased numbers of SMCs, which corresponds to the results found in the scRNA sequencing data based on the identified DEGs.[25]

3.2 Limitations & Future Perspectives

While the results from this research tentatively demonstrate the ability to determine how plaque biology may contribute to DNA methylation, these results have various limitations which should be taken into consideration when interpreting them. One of the largest limitations in this study is the result of having only 492 patients in the methylation dataset, 391 in the BulkRNA dataset and 38 in the scRNA dataset. To find objectively accurate patterns in DNA methylation across patients with a certain plaque phenotype, a significantly larger sample size in necessary to either confirm or deny these findings. So, while the general trends and patterns observed in these results are logical and consistent with literature, a greater population size is necessary for them to be deemed a ‘pattern’ of DNA methylation contributing to plaque phenotype. Similarly, a single-nucleotide polymorphism (SNP) analysis would have allowed us to predict causality of cg26470101 to CHD, but there were not enough patients in the dataset to give this analysis sufficient power, and therefore, causality of cg26470101 methylation in plaque could not be established. Therefore, while it may be the case, as shown in this research, that cg26470101 is implicated in plaque biology, its causality in plaque cannot be extrapolated simply because it is causal in blood leukocyte levels.

Another significant limitation of this research is that by using one CpG as the starting point of the study, this may imply that one CpG acts as an individual entity to determine causality. DNA methylation is known to be a player in the epigenome chromatin modification network, which also involves covalent histone protein post-translational modifications.[26] This includes methylation of several marks and can involve nucleosome remodelling, implying a cross-talk between DNA methylation and post-translational modications.[26] Therefore, using one CpG as the starting point for this research may be inadequate, as it fails to consider that one CpG may reflect the stochastic variation in vasculature microenvironment and plaque composition, rather than being a true driver of atherosclerotic plaque biology.

Since the pipeline used in this research focuses on placing a causal CpG site into the context of plaque biology, it may be of interest for future studies to approach this inversely. For instance, there are known genetic loci that are thought to contribute to atherosclerotic plaque characteristics.[27,28] Instead of determining genes associated with CpGs, the CpGs that map to the genes at these loci could be identified, and then the same analysis could be run with regards to plaque phenotype and sex. This would i) still imply causality of the genes ii) immediately place them into a biological context and would not require a differential gene expression analysis. The genes may also correspond to several CpG sites or a CpG island, and this would therefore eliminate the issue of starting with one CpG.

One of the primary results from this research is the finding that increased methylation of cg26470101 corresponds to patients being more likely to present with fibrous plaques. However, due to the novel nature of the link between DNA methylation and plaque biology, no studies have focused on exploring the relationship between the two, and instead focus on global patterns of DNA hyper- or hypomethylation, or at specific CpG loci identified as significant in atherosclerosis. However, even at the global level, there are conflicting results regarding the status of DNA methylation in atherosclerosis. For instance, where one study found 1858 atherosclerosis-specific methylation sites of which 91% were hypermethylated, another study found that there is a predominant hypomethylation in promoter sites (3997 sites, 84%) in atherosclerotic lesions.[29,30] Interestingly, another study found 1631 atherosclerotic plaque-specific loci which were increasingly methylated as the lesion progresses.[31] Even these conflicting results on such a broad level calls into question what the source of this variation is. This could have several causes, but the difficulties in unifying the results could be due to the known heterogeneity in cellular composition of the atherosclerotic lesions, as well as variation in metabolic processes influencing the local vascular microenvironment.[32] Therefore, while it may be the case that the hypo- or hypermethylation of certain CpG sites contributes to a patient developing a particular plaque phenotype, there is currently no literature that has explored this concept.

Since much variation in the results of DNA methylation patterns likely derives from heterogeneity of the cell composition in the plaque measured, it may be of interest to establish a set of cell-type specific methylation sites within the plaque rather than whole plaque-specific methylation sites. This would enable a better understanding of the contribution of DNA methylation in each cell type in the plaque, thereby also linking the DNA methylation patterns to plaque biology. Packages such as CluBCpG were developed with the goal of exploring variation in CpG methylation patterns in whole genome bisulfite sequencing data, which allowed for the conclusion that CpG methylation patterns in tissue reflect cell type.[33] Therefore, packages such as this one may allow for a better understanding to how plaque methylation patterns are affected by the different cell types in its composition. Lastly, it should be noted that while DNA methylation patterns may be of use to understanding why certain patients develop a particular plaque phenotype, DNA methylation is only one of the biological processes involved in atherosclerotic lesion development. Therefore, future research should focus on combining genetic and epigenetic information, as this is required to successfully understanding what drives atherosclerosis.

The DEGs identified using the bulkRNA dataset were found to be positively expressed with increased cg26470101 methylation, which contradicts the classic tenant of the relationship between DNA methylation and gene expression. This states that increased DNA methylation represses gene expression through recruitment of gene repression related proteins or inhibiting the binding of transcription factors to DNA.[34,35] However, recent research regarding DNA methylation in prostate cancer demonstrated a robust association between DNA hypermethylation and upregulation of gene expression, thereby

challenging this concept.[36] However, this is only a singular study that reports this result and does not directly indicate the need for a paradigm shift within the field. While this does not inherently prove these results to be accurate or implicate them any further in the development of atherosclerosis, it does stand to reason that our current views on DNA methylation may be too simplistic.

cg26470101 is in an intergenic region within the genome. It has also been well-established that hypermethylation in the promoter region of genes can result in gene repression, but only in the last several years has research focused on DNA methylation patterns in different parts of the gene.[37] However, it is still unclear what the effect of DNA methylation in intergenic regions is in general. Research hypothesizes that DNA methylation in intergenic regions in humans may resemble that of plants, where demethylation will lead to reactivation of otherwise repressed repetitive elements, and can lead to genomic instability.[37] In cancer research, intragenic methylation sites have been implicated in disease progression, but the exact mechanisms by which these sites act is unclear. However, due to the fact that CpG sites in intergenic regions overlap with transcriptional initiation sites, they may play an unelucidated functional role.[37] However, exactly how or why this occurs in unclear. Therefore, while research is being done regarding the role of intergenic CpG sites in the context of disease progression, there are many questions that remain unanswered.

4 Conclusion

The primary aim of this research was to determine whether multi-omic dataset integration could be used to associate plaque biological characteristics with DNA methylation. While it was not possible to do so definitively, this research established methods to combining aspects from three different types of datasets, which can be used in future studies. This research found that cg26470101, a CpG site identified as causal to CAD demonstrated increased methylation in fibrous plaques and women, which resulted in identification of 37 DEGs. These DEGs could then be linked to various biological pathways, gene ontologies, and diseases, as well as their expression in ACTA2+ SMCs scRNA sequencing data. Furthermore, it was then found that 59% of the DEGs identified are more expressed in a fibro-cellular plaque phenotype. This demonstrates results consistent with available literature and between the three different datasets used. While various limitations need to be addressed before the analysis can be of any potential clinical value, it did set-up a workflow to eventually enable a more comprehensive understanding of the role of DNA methylation in atherosclerosis and the underlying plaque biology.

5 Methods

R studio (R version 4.1.2) was used to perform all *in silico* data analysis using custom R scripts for this project. Pre-existing packages and pipelines were used and incorporated into these custom R scripts. A script containing the full workflow used in this project can be requested from Mr. Tim Sakkers.

5.1 Data collection and Processing

5.1.1 Athero-Express Biobank

All data used for this research was obtained from the Athero-Express (AE) biobank study. This is an ongoing, longitudinal study that includes patients undergoing arterial endarterectomy in two Dutch hospitals: the University Medical Centre Utrecht (UMCU) and St. Antonius hospital Nieuwegein. Detailed descriptions of the study design and further inclusion criteria, as well as sample collection and processing have been described elsewhere.[38] The clinical information for each patient was also included.

5.2 Methylation Data

5.2.1 DNA Extraction & Methylation Analysis

From the plaque segments and blood samples processed in the manner previously described, DNA was then extracted according to in-house protocols. DNA methylation was measured on the Infinium HumanMethylation450 Beadchip Array (HM450k, Illumina, San Diego, USA). This resulted in DNA from 509 patients, with 503 plaque samples and 97 blood samples. The specific protocols followed are detailed elsewhere.[39]

5.2.2 Quality Control Methylation Data

Quality control was carried out on the 600 samples for which DNA was collected according to a workflow described elsewhere[39], and Figure 6 shows the filtering steps used and the number of samples this left after preprocessing. For this research, only patients who underwent carotid endarterectomy (CEA) in the AtheroExpress biobank were included (n = 492, after quality control and pre-processing).

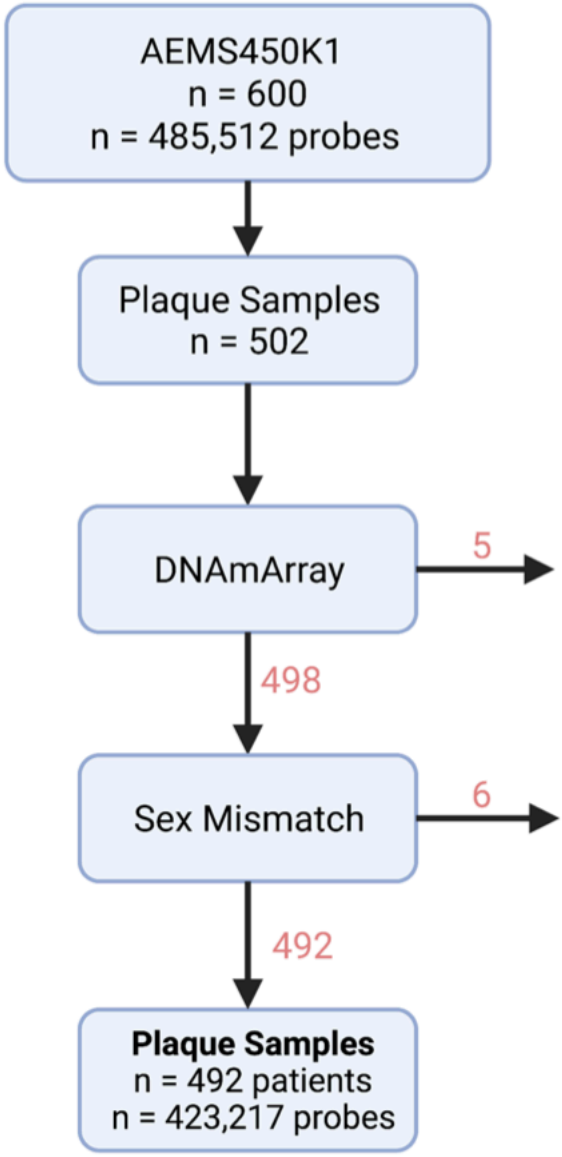

Figure 6. Flowchart showing the steps of data pre-processing, with numbers in red text indicating the number of patients left at each step.

5.2.3 Bulk RNA Data

The methods used to obtain and (pre-)process the bulk RNA data has been described elsewhere (n = 654).[9] This also contains the information regarding the acquisition and (pre-)processing of the transcriptomic clusters.

5.2.4 Single-Cell RNA Data

The methods used to obtain and (pre-)process the single-cell RNA data has been described elsewhere (n = 46).[40]

5.3 Data Analysis

5.3.1 Methylation Data

To generate Table 1 with an overview of patient information included in the methylation dataset, the R package TableOne was used. To determine the correlation between blood and plaque methylation values, the normalized B-values were used to lead to a more intuitive biological result, as the aim of this project was to place the methylation values into a biological context. Regression modelling was performed using the covariates of age, sex, and hospital unless otherwise stated.

5.3.2 BulkRNA Data

Regression modelling regarding the bulkRNA data was performed with plaque phenotype as a covariate. For the differential gene expression analysis, the DEseq2 package was used to obtain the differentially expressed genes, and the EnhancedVolcano package was used to visualize the genes in a volcano plot. A Log2FC and p-value of 10e-5 were used to determine which DEGs had significant changes in their expression which were also statistically significant. To convert the genes from ENSEMBL IDs to EntrezIDs, the org.Hs.eg.db databse was used.

5.3.3 Single Cell RNA Data

For the single-cell data the Seurat package was used to generate all plots.

References

1. Dalen, J. E., Alpert, J. S., Goldberg, R. J. & Weinstein, R. S. The epidemic of the 20th century: Coronary heart disease. *American Journal of Medicine* vol. 127 807–812 (2014).
2. Libby, P. *et al.* Atherosclerosis. *Nat. Rev. Dis. Prim.* **5**, (2019).
3. Herrington, W., Lacey, B., Sherliker, P., Armitage, J. & Lewington, S. Epidemiology of Atherosclerosis and the Potential to Reduce the Global Burden of Atherothrombotic Disease. *Circ. Res.* **118**, 535–546 (2016).
4. Finn, A. V, Nakano, M., Narula, J., Kolodgie, F. D. & Virmani, R. Concept of vulnerable/unstable plaque. *Arteriosclerosis, Thrombosis, and Vascular Biology* vol. 30 (2010).
5. Hellings, W. E., Peeters, W., Moll, F. L. & Pasterkamp, G. From Vulnerable Plaque to Vulnerable Patient: The Search for Biomarkers of Plaque Destabilization. *Trends in Cardiovascular Medicine* vol. 17 (2007).
6. Libby, P. & Pasterkamp, G. Requiem for the 'vulnerable plaque'. *European Heart Journal* vol. 36 (2015).
7. de Jager, S. C. A. *et al.* Preeclampsia and coronary plaque erosion: Manifestations of endothelial dysfunction resulting in cardiovascular events in women. *Eur. J. Pharmacol.* **816**, (2017).
8. Bentzon, J. F., Otsuka, F., Virmani, R. & Falk, E. Mechanisms of plaque formation and rupture. *Circ. Res.* **114**, (2014).
9. Mokry, M. *et al.* Transcriptomic-based clustering of advanced atherosclerotic plaques identifies subgroups of plaques with differential underlying biology that associate with clinical presentation. *medRxiv* 2021.11.25.21266855 (2021) doi:10.1101/2021.11.25.21266855.
10. Vrijenhoek, J. E. P. *et al.* Sex is associated with the presence of atherosclerotic plaque hemorrhage and modifies the relation between plaque hemorrhage and cardiovascular outcome. *Stroke* **44**, (2013).
11. Yahagi, K., Davis, H. R., Arbustini, E. & Virmani, R. Sex differences in coronary artery disease: Pathological observations. *Atherosclerosis* vol. 239 (2015).
12. Lansky, A. J. *et al.* Gender and the extent of coronary atherosclerosis, plaque composition, and clinical outcomes in acute coronary syndromes. *JACC Cardiovasc. Imaging* **5**, (2012).
13. Man, J. J., Beckman, J. A. & Jaffe, I. Z. Sex as a Biological Variable in Atherosclerosis. *Circ. Res.* (2020) doi:10.1161/CIRCRESAHA.120.315930.
14. Fernández-Sanlés, A., Sayols-Baixeras, S., Subirana, I., Degano, I. R. & Elosua, R. Association between DNA methylation and coronary heart disease or other atherosclerotic events: A systematic review. *Atherosclerosis* vol. 263 325–333 (2017).
15. Tabaei, S. & Tabaee, S. S. DNA methylation abnormalities in atherosclerosis. *Artificial Cells, Nanomedicine and Biotechnology* vol. 47 (2019).
16. Agha, G. *et al.* Blood Leukocyte DNA Methylation Predicts Risk of Future Myocardial Infarction and Coronary Heart Disease. *Circulation* **140**, (2019).
17. Dai, Y., Chen, D. & Xu, T. DNA Methylation Aberrant in Atherosclerosis. *Front. Pharmacol.* **13**, (2022).
18. Bennett, B. J., Wang, S. S., Wang, X., Wu, X. & Lusis, A. J. Genetic regulation of atherosclerotic plaque size and morphology in the innominate artery of hyperlipidemic mice. *Arterioscler. Thromb. Vasc. Biol.* **29**, 348–355 (2009).
19. Kuleshov, M. V *et al.* Enrichr: a comprehensive gene set enrichment analysis web server 2016 update. *Nucleic Acids Res.* **44**, W90-7 (2016).
20. Larsen, J. B. & Hvas, A.-M. Fibrin clot properties in coronary artery disease: new determinants and prognostic markers. *Polish Arch. Intern. Med.* **131**, (2021).
21. Kaur, S., Jayakumar, K. & Kartha, C. C. The potential of circulating endothelial progenitor cells to form colonies is inversely proportional to total vascular risk score in patients with coronary artery disease. *Indian Heart J.* **59**, 475–481 (2007).
22. Domouzoglou, E. M. *et al.* Fibroblast growth factors in cardiovascular disease: The emerging

role of FGF21. *Am. J. Physiol. Heart Circ. Physiol.* **309**, H1029-38 (2015).
23. Rosenson, R. S. *et al.* Dysfunctional HDL and atherosclerotic cardiovascular disease. *Nat. Rev. Cardiol.* **13**, 48–60 (2016).
24. Olie, R. H., van der Meijden, P. E. J. & Ten Cate, H. The coagulation system in atherothrombosis: Implications for new therapeutic strategies. *Res. Pract. Thromb. Haemost.* **2**, 188–198 (2018).
25. Hellings, W. E. *et al.* Intraobserver and interobserver variability and spatial differences in histologic examination of carotid endarterectomy specimens. *J. Vasc. Surg.* **46**, 1147–1154 (2007).
26. Jeltsch, A., Broche, J. & Bashtrykov, P. Molecular Processes Connecting DNA Methylation Patterns with DNA Methyltransferases and Histone Modifications in Mammalian Genomes. *Genes* vol. 9 (2018).
27. van der Laan, S. W. *et al.* Genetic Susceptibility Loci for Cardiovascular Disease and Their Impact on Atherosclerotic Plaques. *Circ. Genomic Precis. Med.* **11**, e002115 (2018).
28. Aherrahrou, R. *et al.* Genetic Regulation of Atherosclerosis-Relevant Phenotypes in Human Vascular Smooth Muscle Cells. *Circ. Res.* **127**, 1552–1565 (2020).
29. Zaina, S. *et al.* DNA Methylation Map of Human Atherosclerosis. *Circ. Cardiovasc. Genet.* **7**, 692–700 (2014).
30. Aavik, E. *et al.* Global DNA methylation analysis of human atherosclerotic plaques reveals extensive genomic hypomethylation and reactivation at imprinted locus 14q32 involving induction of a miRNA cluster. *Eur. Heart J.* **36**, 993–1000 (2015).
31. Valencia-Morales, M. del P. *et al.* The DNA methylation drift of the atherosclerotic aorta increases with lesion progression. *BMC Med. Genomics* **8**, 7 (2015).
32. Aavik, E., Babu, M. & Ylä-Herttuala, S. DNA methylation processes in atherosclerotic plaque. *Atherosclerosis* **281**, 168–179 (2019).
33. Scott, C. A. *et al.* Identification of cell type-specific methylation signals in bulk whole genome bisulfite sequencing data. *Genome Biol.* **21**, 156 (2020).
34. Moore, L. D., Le, T. & Fan, G. DNA Methylation and Its Basic Function. *Neuropsychopharmacology* **38**, 23–38 (2013).
35. Li, Y., Chen, X. & Lu, C. The interplay between DNA and histone methylation: molecular mechanisms and disease implications. *EMBO Rep.* **22**, e51803 (2021).
36. Rauluseviciute, I., Drabløs, F. & Rye, M. B. DNA hypermethylation associated with upregulated gene expression in prostate cancer demonstrates the diversity of epigenetic regulation. *BMC Med. Genomics* **13**, 6 (2020).
37. Shenker, N. & Flanagan, J. M. Intragenic DNA methylation: implications of this epigenetic mechanism for cancer research. *Br. J. Cancer* **106**, 248–253 (2012).
38. Verhoeven, B. A. N. *et al.* Athero-express: Differential atherosclerotic plaque expression of mRNA and protein in relation to cardiovascular events and patient characteristics. Rationale and design. *Eur. J. Epidemiol.* **19**, (2004).
39. Siemelink, M. A. *et al.* Smoking is Associated to DNA Methylation in Atherosclerotic Carotid Lesions. *Circ. Genomic Precis. Med.* **11**, (2018).
40. Depuydt, M. A. C. *et al.* Microanatomy of the Human Atherosclerotic Plaque by Single-Cell Transcriptomics. *Circ. Res.* **127**, 1437–1455 (2020).

Supplemental Tables

Table S1. Top 37 DEGs identified via BulkRNA sequencing data. Increased expression of these genes is associated with increased methylation of cg26470101.

GENE ABBREVIATION	GENE
GSTM5	Glutathione S-Transferase Mu 5
AADACL3	Arylacetamide Deacetylase Like 3
NET1	Neuroepithelial Cell Transforming 1
ABCA4	ATP-binding cassette, sub-family A, member 4
FIBIN	Fin Bud Initiation Factor Homolog
ABCD3	ATP Binding Cassette Subfamily Member 3
C12ORF75	Chromosome 12 Open Reading Frame 75
GLT8D2	Glycosyltransferase 8 Domain Containing 2
KCNA5	Potassium Voltage-Gated Channel Subfamily A Member 5
RERGL	RERG-like
TMEM106C	Transmembrane protein 106C
SYNM	Synemin
ECRG4	ECRG4 Augurin Precursor
FRZB	Frizzled Related Protein
PID1	Phosphotyrosine Interaction Domain Containing 1
TUBB1	Tubulin Beta-1 Class VI
ADCY5	Adenylate Cyclase 5
DNAJC19	DnaJ Heat Shock Protein Family (Hsp40) Member C19
KCNAB1	Potassium Voltage-Gated Channel Subfamily A Regulatory Beta Subunit 1
NR1D2	Nuclear Receptor Subfamily 1 Group D Member 2
PROS1	Protein S
CPE	Carboxypeptidase E
NPNT	Nephronectin
PF4	Platelet Factor 4
RASL11B	Ras-like Family 11 Member B
PRDM6	PR/SET Domain 6
PLN	Phospholamban
SLC22A3	Solute-carrier Family 22 Member 3
SMOC2	SPARC-related modular calcium-binding protein 2
DLX5	Distal-less Homeobox 5
SUGCT	Succinyl-CoA:Glutarate-CoA Transferase
CRISPLD1	Cystein Rich Secretory Protein LCCL Domain Containing 1
BEX1	Brain Expressed X-linked 1
LDOC1	LDOC1 Regulator of NF-kB Signalling
MAOB	Monoamine Oxidase B
NAP1L3	Nucleosome Assembly Protein 1 Like 3
TCEAL7	Transcription Elongation Factor A Like 7

Table S2. Gene enrichment analysis for pathways linked to the 37 identified DEGs.

DATABASE	PATHWAY	ADJUSTED P-VALUE
Msigdb Hallmark 2020	*Angiogenesis*	*0.2582*
	Bile Acid Metabolism	*0.1613*
	Coagulation	*0.1613*
	IL-6/Jak/STAT3 Signalling	*0.3108*
	Peroxisome	*0.3108*
	UV Response Dn	*0.3108*
	Mitotic Spindle	*0.3108*
	Xenobiotic Metabolism	*0.3108*
	Oxidative Phosphorylation	*0.3108*
KEGG 2021 Human	*ABC Transporters*	*0.1557*
	Cocaine Addiction	*0.1557*
	Phenylalanine Metabolism	*0.2394*
	Histidine Metabolism	*0.2581*
	Amphetamine Addiction	*0.1906*
	Gap Junction	*0.1906*
	Dilated Cardiomyopathy	*0.1906*
	Drug Metabolism	*0.1945*
	Tyrosine metabolism	*0.2957*
	Serotonergic Synapse	*0.1945*
Reactome 2016	*Abacavir transmembrane transport*	*0.1285*
	Common Pathway of Fibrin Clot Formation	*0.08943*
	Organic cation transport	*0.1285*
	Transport of gamma-carboxylated protein precursors from the endoplasmic reticulum to the Golgi apparatus	*0.1285*
	Abacavir transport and metabolism	*0.1285*
	Removal of aminoterminal propeptides from gamma-carboxylated proteins	*0.1285*
	Gamma-carboxylation of protein precursors	*0.1285*
	Adenylate cyclase activating pathway	*0.1285*
	Gamma-carboxylation, transport, and amino-terminal cleavage of proteins	*0.1333*
	Formation of Fibrin Clot (Clotting Cascade)	*0.09329*
Wikipathway 2021 Human	*Dopamine Metabolism*	*0.1728*
	Major receptors targeted by epinephrine and norepinephrine	*0.1728*
	Platelet-mediated interactions with vascular and circulating cells	*0.1728*
	Gastric cancer network 1	*0.1728*
	16p11.2 distal deletion syndrome	*0.1728*
	Nuclear receptors in lipid metabolism and toxicity	*0.1728*
	Nuclear receptors	*0.1728*
	Tryptophan metabolism	*0.1728*
	Envelope proteins and their potential roles in EDMD physiopathology	*0.1728*
	Exercise-induced circadian regulation	*0.1728*

Table S3. Gene enrichment analysis for gene ontology linked to the 37 identified DEGs.

DATABASE	ONTOLOGY	ADJUSTED P-VALUE
GO Biological Process 2021	*Serotonin transport*	*0.1137*
	Serotonin uptake	*0.1137*
	Atrial cardiac muscle cell membrane repolarization	*0.1137*
	Membrane repolarization during atrial cardiac muscle cell action potential	*0.1137*
	Positive regulation of fibroblast growth factor receptor signalling pathway	*0.1137*
	Bundle of His cell action potential	*0.1137*
	Dopamine catabolic process	*0.1137*
	Cell-cell adhesion mediated by integrin	*0.1137*
	Regulation of relaxation of cardiac muscle	*0.1137*
	Norepinephrine transport	*0.1137*
GO Molecular Function 2021	*ATPase inhibitor activity*	*0.09965*
	CXCR3 chemokine receptor binding	*0.09965*
	All-trans retinal binding	*0.09965*
	11-cis retinal binding	*0.09965*
	Phosphatidylethanolamine flippase activity	*0.09965*
	Monoamine transmembrane transporter activity	*0.09965*
	Retinal binding	*0.09965*
	Adenylate cyclase binding	*0.09965*
	Aldo-keto reductase (NADP) activity	*0.09965*
	Outward rectified potassium channel activity	*0.09965*

Table S4. Gene enrichment analysis for diseases linked to the 37 identified DEGs.

DATABASE	DISEASE	ADJUSTED P-VALUE
GWAS Catalog 2019	*Neuritic plaques or neurofibrillary tangles (pleiotropy)*	*0.06339*
	Neuritic plaques or neurofibrillary tangles or cerebral amyloid angiopathy (pleiotropy)	*0.06339*
	Aging traits	*0.06339*
	Two-hour glucose challenge	*0.06339*
	Cognitive flexibility	*0.06339*
	Waist-to-hip circumference ratio (dietary energy interaction)	*0.06339*
	Cardiac structure and function	*0.06339*
	Response to citalopram or escitalopram and depression	*0.06339*
	Percent mammographic density	*0.06339*
	Corrected insulin response	

Supplemental Figure

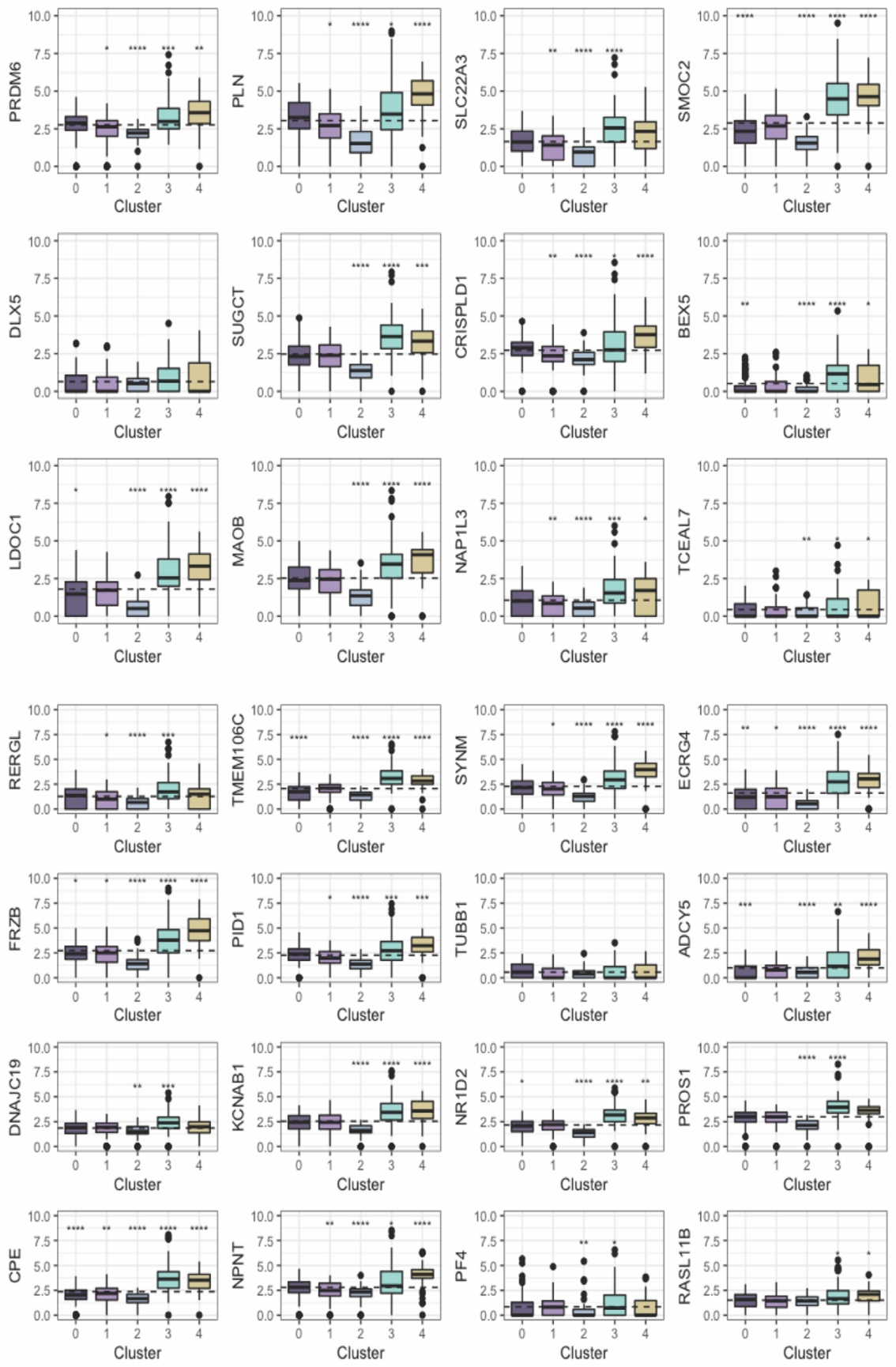

Figure S1. Boxplots showing 28 DEGs identified from the BulkRNA sequencing data.

Phenotypic Modulation of Plaque Cells

Astrid Hofman
Prof. Dr. Ir. Hester den Ruijter, PhD
September 26th, 2022

Abstract

Aims: The progression of atherosclerosis is characterized by an accumulation of smooth muscle cells (SMCs) in the *intima* of the vessel. They can exist as spindle-shaped (S)-SMCs or rhomboid (R)-SMCs, where S100A4 is a marker of the R-SMCs and involved in the phenotypic transition from S-SMC to R-SMC. This study aimed to investigate whether i) lipopolysaccharide (LPS), a well-known endotoxin that signals similarly to S100A4 could induce this phenotypic transition ii) whether S100A4 could induce a phenotypic switch in human coronary artery smooth muscle cells (HCASMCs) and plaque cells (Plaque cells), which are suspected to be transdifferentiated vascular SMCs.

Method & Results: HCASMCs and Plaque cells were stimulated with LPS to induce nuclear factor (NF)-kB activation. HCASMCs and Plaque cells were stimulated in complete medium, FCS-depletion medium, and starvation medium for 96 hours to observe any morphological changes. When stimulated in FCS-depletion medium, some of the HCASMCs stimulated with LPS or LPS/platelet-derived growth factor (PDGF)-BB demonstrate a switch from an elongated morphology to a more compact, small morphology when compared to the control and earlier time points for the same condition. Plaque cells do not demonstrate the same results. It was not possible to induce NF-ϰB activation with S100A4 in either cell type.

Future Perspectives & Conclusion: While the ability of LPS to induce a phenotypic switch of the HCASMCs could not be quantified, changes in morphology were observed. This study validated an experimental set-up for future experiments to provide better quantitative results and thereby elucidate the molecular mechanisms contributing to SMC phenotypic modulation.

Plain-Text Summary

Atherosclerosis is a common, chronic condition which can lead to various clinical events, such as a heart attack or a stroke. In atherosclerosis, there is a build-up of fatty substances such as cholesterol in the arteries, which form a 'plaque' within the walls of the arteries. These plaques are composed of many different cell types, each with their own function(s). One of these cell types is the vascular smooth muscle cell. In the healthy artery, vascular smooth muscle cells are responsible for maintaining the shape of the artery so that blood can pass through and maintaining blood pressure. Here, they take on a 'spindle-shaped' form. In atherosclerosis, there is a build-up of smooth muscle cells in the inner layer of the artery. They play an important role in healing the artery wall when it is damaged due to atherosclerotic processes. In response to this injury, the vascular smooth muscle cells can change their form, and they can detach from the vessel wall, which means they are now 'modulated' vascular smooth muscle cells. The ability to change forms is due to a process referred to as 'cellular plasticity', which allows cells to change their form.

Recently, it has also been shown that it is possible to grow cells that are derived from atherosclerotic plaques in the laboratory. These plaque cells share a remarkable amount of characteristics with vascular smooth muscle cells and are thought to come from the modulated vascular smooth muscle cells after undergoing various molecular processes. By growing these cells in the laboratory, we have developed a relevant, human model for studying the capacity for these cells to change form, similarly to the vascular smooth muscle cells.

Vascular smooth muscle cells and their ability to change forms are heavily involved in the development of atherosclerotic plaques, making it of interest to study how these processes occur. Recent research has shown that there are 2 sub-populations of these vascular smooth muscle cells. One of these sub-populations is characterized by a long, thin shape, and the other is characterized by a rhomboid shape. Researchers have found that you can induce the long, thin vascular smooth muscle cells to transition to the rhomboid shape when you give it a certain protein. When smooth muscle cells take on this rhomboid shape, they acquire more inflammatory properties, and are thought to be able to switch into other cell types more easily.

What we wanted to determine with this research is whether it would also be possible to stimulate our plaque cells to switch to the rhomboid form, which would allow us to better understand these cells and their ability to switch to a different cell type, and this would in turn help us understand the progression of atherosclerosis better. We found that when you stimulate plaque cells with a component found in bacteria, that they can switch shape. We have yet to determine whether this is due to the stimulation or whether it is due to external factors but serves as a jumping off platform for future studies.

1. Introduction

Atherosclerosis is a systemic, inflammatory condition which can result in various clinical consequences and is characterized by an accumulation of fibro-fatty material in the arterial *intima*, resulting in formation of atherosclerotic plaques.[1–4] Plaques can induce clinical events through erosion of a stable plaque that occludes the arterial lumen, or due to thrombotic events mediated by the acute rupture of an unstable plaque.[4] Post-mortem histological studies have identified various characteristics that precede plaque rupture and therefore describe unstable plaques.[4] These qualities include: i) a large number of cells positive for macrophage markers, such as CD68; ii) the presence of a large necrotic core filled with lipids; and iii) a thin or fragmented fibrous cap, identified by α-actin (ACTA2)-positive cells, which are thought to be derived from vascular SMCs (VSMCs).

In healthy adult vessels, VSMCs reside in the *tunica media* of the blood vessel wall, where they serve to modulate blood vessel diameter, regulate blood flow distribution and blood pressure and produce extracellular matrix (ECM).[5–7] VSMCs retain a high degree of cellular plasticity, allowing them to alter their phenotype based on local environmental stimuli such as injury.[5,8,9] In the context of atherosclerosis, VSMCs play a role in remodeling the arterial wall to sustain blood flow in arteries damaged due to atherosclerotic processes. To do so, VSMCs transdifferentiate from the basal contractile-like phenotype to a 'synthetic' phenotype.[5]

In disease states such as vascular injury or atherosclerosis, VSMCs undergo phenotypic switching, a process mediated by myocardin (MYOCD) expression.[6] As a response to vascular injury or in the atherosclerotic plaque, a loss of MYOCD expression leads to decreased expression of SMC-specific markers including but not limited to: MYH11, 22-kDa SMC lineage-restricted protein (SM22α) and α-SMA.[5,6,10] Upon loss of MYOCD and thereby the SMC-specific markers, modulated-VSMCs may undergo a process, governed by Krüppel-like factor 4 (KLF4), which facilitates VSMC transdifferentiation.[3,5,6,9] This KLF4-program is thought to give rise to smooth muscle-like plaque cells which may be capable of transdifferentiation towards other cell lineages involved in vascular disease and thereby contributing to plaque progression.[5,6]

Single-cell transcriptomics has shown that these plaque cells demonstrate a close resemblance to $ACTA2^{+}$ plaque SMCs and specifically to SMC-derived myofibroblasts. These plaque cells can be cultured using an outgrowth method deriving the cells from human atherosclerotic lesions, thus developing a relevant human *in vitro* system for studying atherosclerotic mechanisms. It is thought that the culture of these plaque cells may provide a group of mesenchymal-like cells that retain the capacity to transdifferentiate through acquisition of a pro-inflammatory phenotype, which causes them to lose expression of SMC-specific markers and potentially acquire markers associated with other cell types.

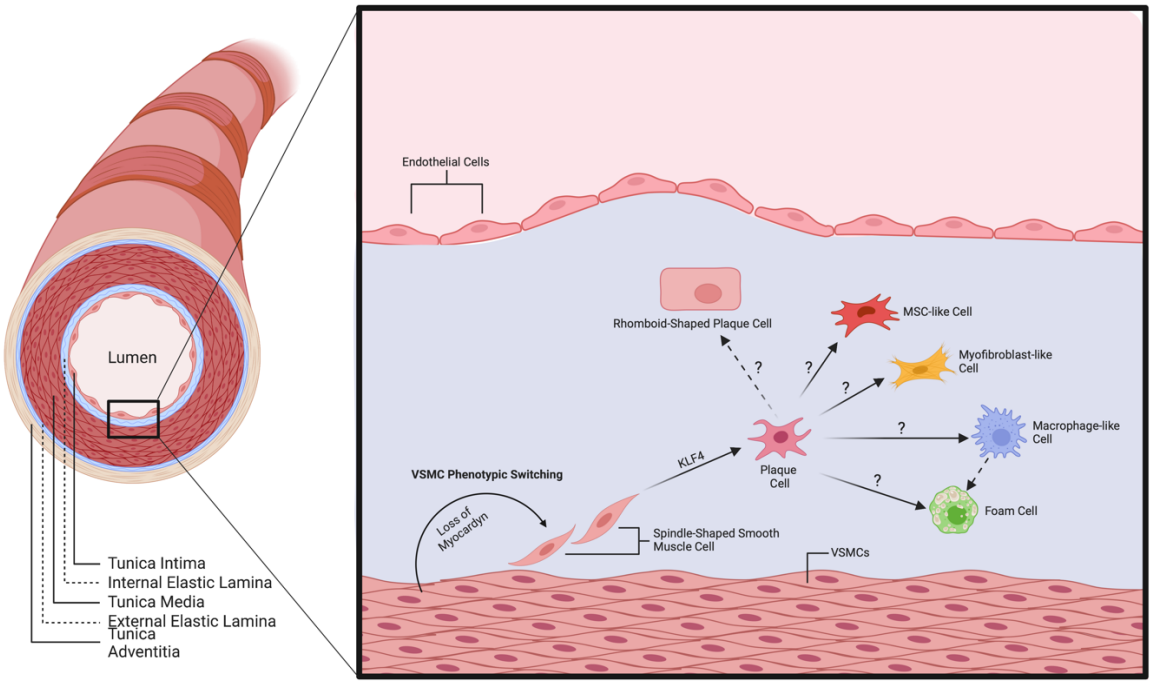

Figure 1. Visualization of the proposed mechanism of transdifferentiation of vascular smooth muscle cells to plaque cells. Adapted from Buono et al.[6]

In recent years, VSMC plasticity has been found to be heavily involved in the development of atherosclerotic plaques, making it interesting to further elucidate the mechanisms underlying this transdifferentiation process. A recent study [11] has isolated 2 sub-populations of SMCs: spindle-shaped (S-SMCs) and rhomboid SMCs (R-SMCs).[11–13] R-SMCs are characterized by increased proliferative, migratory, and proteolytic capacities compared to S-SMCs, as well as an increased expression of S100A4.[13] S100A4 was found to be barely detectable in coronary artery media, and expressed is significantly increased in SMCs found in atheromatous and restenotic artery lesions.[13] Additionally, silencing of S100A4 in R-SMCs decreased cell proliferation, further implying a functional role for S100A4.[13] S100A4 has both intra- and extracellular functions, where extracellular S100A4 is known to trigger pro-inflammatory processes and serves as an activator of inflammatory molecules such as interleukin (IL)-1, IL-6, tumour necrosis factor (TNF-α), and matrix metalloproteinases (MMPs).[11] It has been shown that *in vitro* S100A4 exists in an oligomeric conformation, where is associates with pro-inflammatory pathway receptors such as the receptor for advanced glycation end products (RAGE), toll-like receptor 4 (TLR4), and epidermal growth factor receptor (EGFR).[11] The transition from the S-SMC phenotype to the R-SMC phenotype has been associated with NF-κB activation and changes in MMPs and their inhibitors. Sakic et al. recently showed that when stimulated with both oligomeric S100A4 (oS100A4) and platelet-derived growth factor (PDGF)-BB, which is known to stimulate SMC differentiation, a complete phenotypic transition from the S-SMC to R-SMC phenotype occurs in porcine SMCs.[11] Additionally, it was also found that when stimulated with PDGF-BB, SMCs also obtain a more rhomboid phenotype.[14]

This research aims to build off both these results by stimulating human smooth muscle cells and human plaque cells to determine the capacity of each cell type to switch to a "rhomboid" phenotype. The research by Sakic et al. uses S100A4, which they show induces phenotypic switching through TLR-4 dependent activation of the NF-κB pathway.[11] However, another well-known and widely available substrate known to activate TLR4-dependent NF-κB is lipopolysaccharide (LPS), which has also been shown to upregulate VSMC proliferation.[15–17] Enhanced proliferation is associated with the dedifferentiated VSMC phenotype, and therefore it stands to reason that LPS may also be capable of inducing a switch from the spindle-shaped to the rhomboid SMC phenotype.

This research aims to determine the switching capacity of human SMCs and plaque cells using LPS and S100A4 and stimulate them to a rhomboid phenotype. This aids in understanding the mechanisms through which SMCs and plaque cells undergo phenotypic modulation, and thereby understanding a prominent pathological process involved in atherosclerosis progression. It was determined that when stimulated with LPS, NF-κB signalling could be activated in both SMCs and plaque cells, and when cultured in FCS-depletion medium some morphological changes were observed in the SMCs. However, it was not possible to activate NF-κB using S100A4, likely due to its monomeric conformation.

2. Results

2.1. LPS can induce NF-κB activation in human aortic smooth muscle cells and plaque cells

This pilot study was performed to determine whether NF-κB could be activated using lipopolysaccharide (LPS) in MRC-5 fibroblasts (MRC-5s), human microvascular epithelial cells (HMECs), human artery smooth muscle cells (HASMCs), and plaque cells. Each cell type wes treated with either LPS or LPS and PDGF-BB for 1 hour and then investigated via immunofluorescence. In all cell types, when treated with LPS 10 ug/mL and with LPS 10ug/mL and PDGF-BB 30 ng/mL, most cells display translocation of NF-κB to the nuclei (Figure 2, Figure S1). While, when stimulated with LPS at 1 ug/mL, the HASMCs and Plaque cells show NF-κB translocation in the majority of cells, thereby demonstrating activation of the NF-κB pathway. In control conditions for all cell types, there is no NF-κB translocation to the nucleus observed (Figure 2, Figure S1). To determine activation of the NF-κB pathway, the staining dilutions used were optimized (Figure S2).

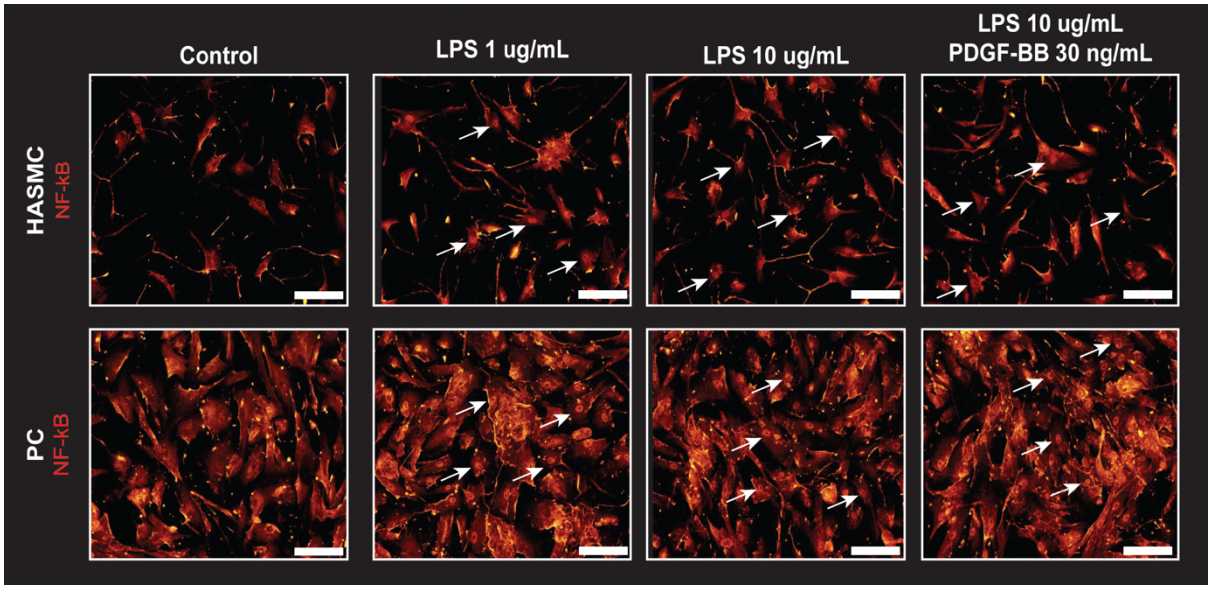

Figure 2. LPS-induced NF-κB activation in HASMCs and plaque cells taken at 10x magnification. HASMCs and Plaque cells stimulated with either LPS at 1 ug/mL, LPS at 10 ug/mL or LPS at 10 ug/mL and PDGF-BB at 30 ng/mL. Activation of the NF-κB pathway is shown by illuminated nuclei. Scale bar: 200 µm. Abbreviations: HASMC: human aortic smooth muscle cells; PC: plaque cells; LPS: Lipopolysaccharide; PDGF-BB: platelet-derived growth factor BB; NF-κB: Nuclear transcription factor kappa B.

2.2. LPS can induce morphological changes in human aortic smooth muscle cells and plaque cells cultured in FCS-depletion medium

To investigate whether HCASMCs and plaque cells could display phenotypic switching when stimulated with LPS/PDGF-BB, cells were stimulated with LPS, LPS/PDGF-BB, or PDGF-BB alone and observed over 96 hours. To also evaluate the effect of different medium compositions on the phenotypic switch, stimulation was carried out in complete medium, FCS depletion medium, and starvation medium (composition in section 5.1.2) were used to culture the cells.

In complete medium, across all time points and conditions, the cells remain maintained the same morphology, as elongated and spindle shaped. It does appear that the plaque cells stimulated with PDGF-BB exhibit greater proliferative capacity compared to the HCASMCs at the same time point (Figure S4).

The HCASMCs cultured in depletion medium demonstrate less elongated morphology when compared to the control and PDGF-BB stimulated conditions (Figure 3). In the LPS/PDGF-BB stimulated condition, after 24 hours there is a marked change towards a shorter, more compact cell shape (Figure 3Ae-3Ah). This change is also evident in the LPS-stimulated cells after 48 hours (Figure 3Af). At the 96-hour time point, some cells remain spindle-shaped, but the majority in both the LPS and LPS/PDGF-BB stimulated cells, there is a switch to a more compact cell-shape, compared to both the control and PDGF-BB stimulated conditions (Figure 3). The plaque cells cultured in depletion medium do not demonstrate a change in morphology as dramatic as the HCASMCs, but in the LPS/PDGF-BB stimulated cells there are various cells that display a more compact morphology. Notably, the LPS-stimulated cells do not show any change in morphology at the 96-hour mark and remain elongated (Figure 3Bh).

For the HCASMCs cultured in starvation medium, the control condition, LPS-, and PDGF-BB stimulated conditions do not display any changes in cell morphology in any timepoint. In the LPS/PDGF-BB stimulated cells, there appears to be a change in morphology starting at 72 hours and continuing to the 96-hour timepoint. The plaque cells cultured in starvation medium do not display any changes in morphology over any of the conditions or timepoints but do have a significant number of apoptotic bodies or debris present.

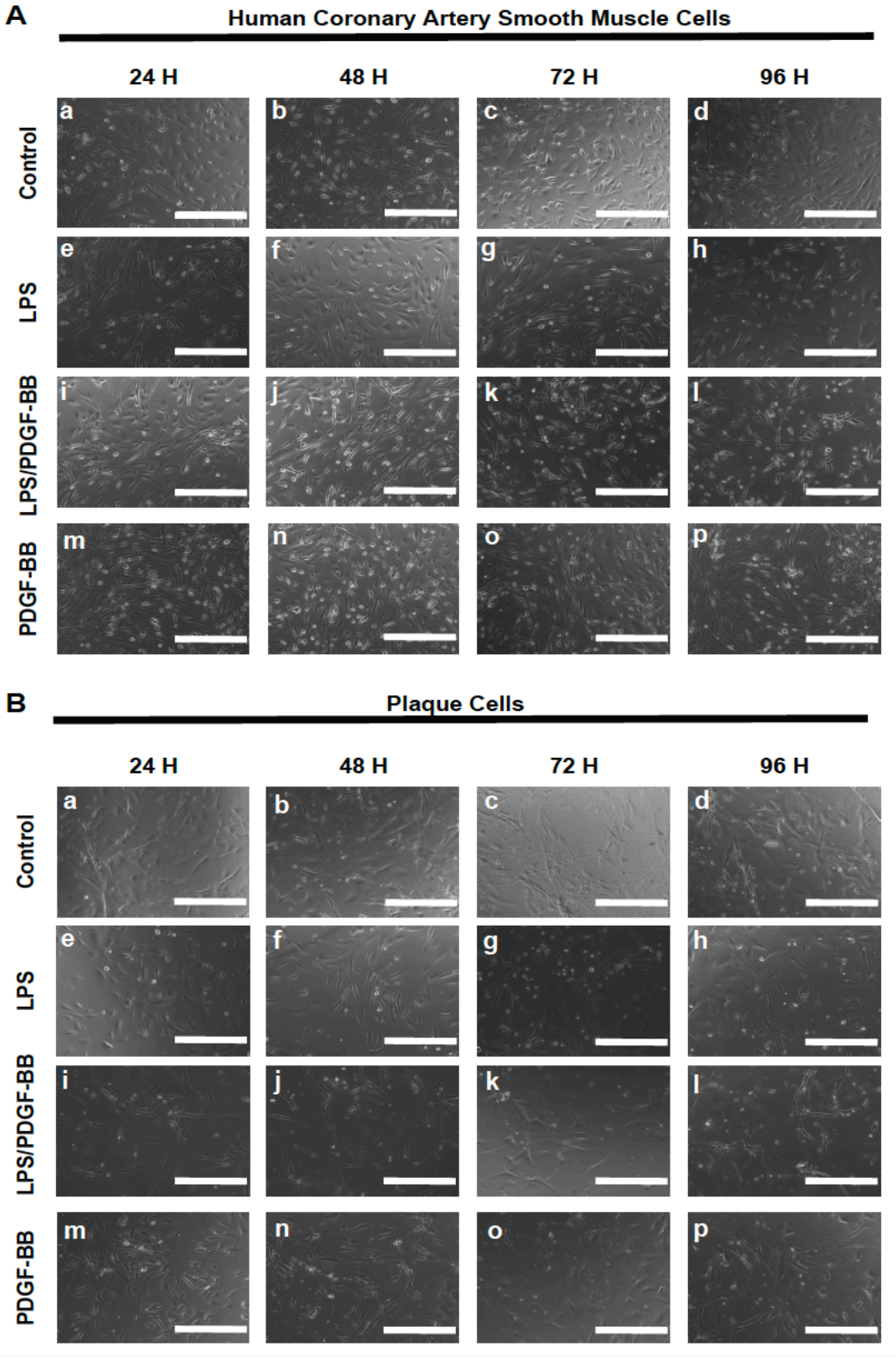

Figure 3. Morphological Changes in HCASMCs cells and plaque cells cultured in FCS-depletion medium taken at 10x magnification. A. Process of morphological changes starting 24 hours post-stimulation of the human coronary artery smooth muscle cells. Demonstrates a switch to a shorter, more compact cell in the LPS and LPS/PDGF-BB conditions starting at 72 hours and continuing until the 96-hour timepoint. B. Process of morphological changes starting 24 hours post-stimulation of the plaque cells. This demonstrates no clear change in morphology between the time points. Scale bar: 400 µm. Abbreviations: LPS: Lipopolysaccharide; PDGF-BB: platelet-derived growth factor BB; NF-κB: Nuclear transcription factor kappa B; H: hours.

2.3. S100A4 stimulation is unable to induce NF-κB activation

To determine activation of the NF-κB pathway in both HCASMCs and Plaque cells using commercial S100A4, cells were stimulated with either S100A4, S100A4/PDGF-BB, or LPS/PDGF-BB, serving as a positive control, and subsequently analysed using immunofluorescence. This revealed that in both the HCASMCs and plaque cells, stimulation with S100A4 alone or in combination with PDGF-BB did not cause translocation of NF-κB to the nuclei. When stimulated with LPS/PDGF-BB, however, there is a clear activation of the NF-κB pathway (Figure 4). To determine why S100A4 did not activate the NF-κB pathway, the conformation of the S100A4 protein was determined running as SDS-PAGE gel. This revealed that commercial S100A4 has a monomeric structure, as indicated by the band at 15 kDa (Figure S5). Sakic et al. determined that to activate NF-κB signalling, the S100A4 protein had to be an oligomeric form, explaining the lack of activation observed in both HCASMCs and plaque cells (Figure 4).

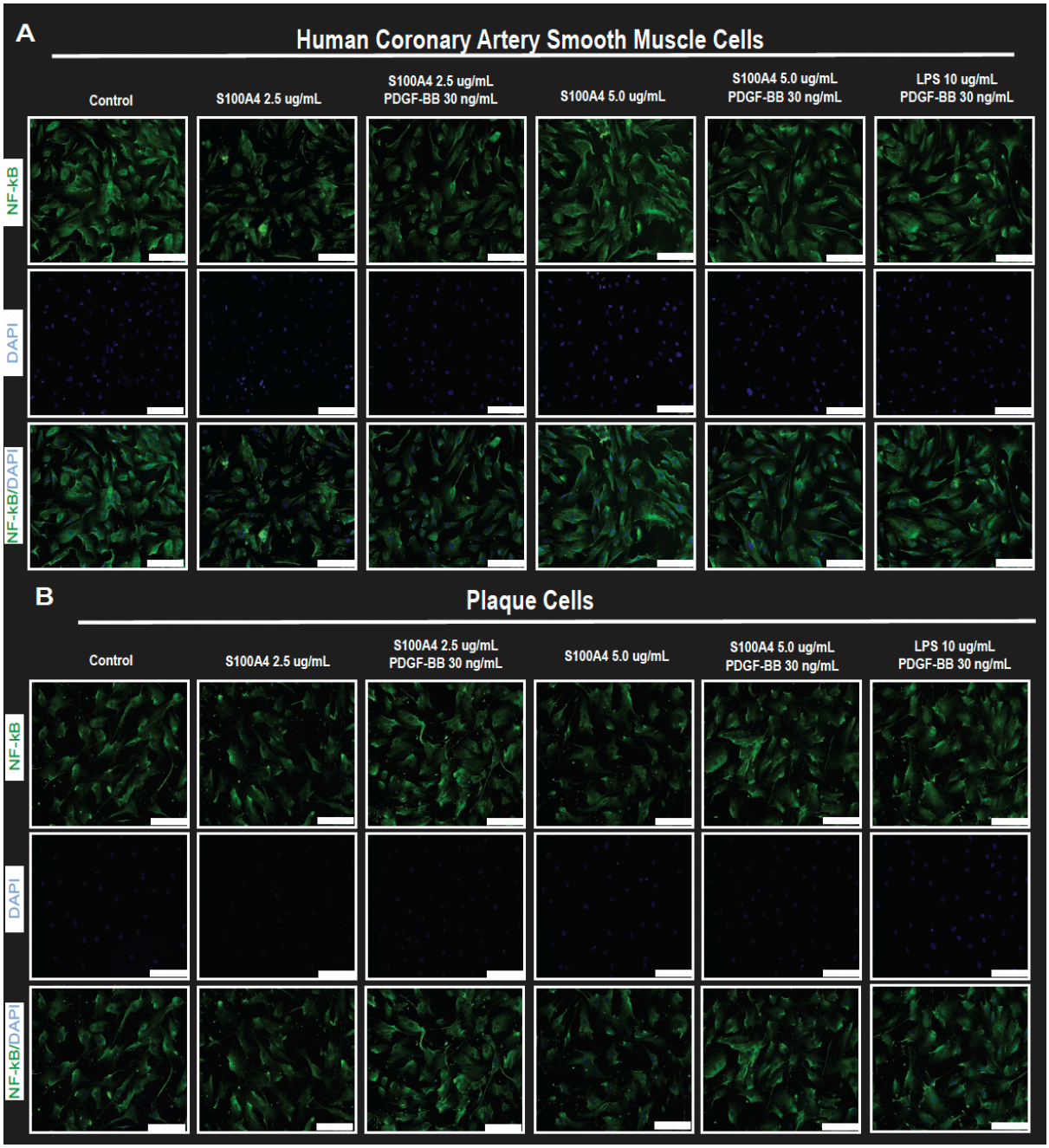

Figure 4. S100A4-Induced NF-κB *a*ctivation of HCASMCs and Plaque cells taken at 20x Magnification. A. Showing the different conditions for S100A4 activation in HCASMCs. Demonstrates that commercially purchased S100A4 is unable to activate the NF-κB pathway. B. Showing the different conditions for S100A4 activation in plaque cells. Demonstrates that commercially purchased S100A4 is unable to activate the NF-κB pathway. Scale bar: 200 µm. Abbreviations: LPS: Lipopolysaccharide; PDGF-BB: platelet-derived growth factor BB; NF-κB: Nuclear transcription factor kappa B.

3. Discussion

The transition from S-SMC to a R-SMC phenotype is characterized by decreased markers of SMC differentiation, increased proliferation and migration, MMP production and their inhibitors.[22] While the signalling pathways and molecular processes involved in this phenotypic modulation are not completely elucidated. Several studies have shown that LPS is involved in VSMC proliferation, a process implicated in atherosclerotic plaque formation.[4,15,16,23] LPS is thought to exert an effect on VSMC proliferation mediated by the TLR4/Rac1/Akt signalling pathway and play a role in LPS-mediated phenotypic modulation.[15] LPS has been found to increase the expression and protein levels of myosin-heavy chain (MYH)-11 and SM22α.[15] Additionally, the downregulation of TLR4 or Rac1 inhibits LPS-mediated VSMC differentiation, implying a role of this signalling pathway in the proliferation and phenotypic modulation of VSMCs.[15] Lastly, NF-κB activation is known to play a role in LPS-induced VSMC proliferation.[16]

To determine whether LPS could activate NF-κB and induce any morphological changes, we stimulated HCASMCs and plaque cells using different concentrations of LPS. HCASMCs cultured in FCS-depletion medium and stimulated with LPS or LPS/PDGF-BB show morphological changes starting at 72 hours and continuing to 96 hours, both compared to the control condition and earlier time points (Figure 3). The HCASMCs became considerably more compact and less elongated when compared to both earlier time points in the same conditions and the control condition and the PDGF-BB stimulated condition. Plaque cells cultured in the same FCS-depletion medium have potentially demonstrated a change in morphology at 96 hours when stimulated with LPS/PDGF-BB, but less dramatic than in the HCASMCs. This may occur since plaque cells may be transdifferentiated VSMCs, thus requiring different stimuli *in vitro* to modulate their phenotype. No morphological changes were observed when both the HCASMCs and plaque cells were cultured in complete or starvation medium. Therefore, it stands to reason that the FCS-depletion medium may play a part in the morphological changes observed, but it is unclear what this contribution is or how it arises. It may be that FCS-depletion medium places the cells under enough stress to trigger a survival response, whereas the complete medium composition and starvation medium composition stimulate growth and apoptosis, respectively. This, in combination with the known activation of NF-κB and release of pro-inflammatory cytokines due to LPS stimulation may somehow also cause a change in the HCASMC morphology. However, this is purely speculative. The role of LPS on VSMC proliferation has been relatively well-established, and as one of the characteristics of R-SMCs is increased proliferative capacity, this could be another method to determine changes in morphology. Again, due to the visual inspection of transmitted light images, it is difficult to quantify proliferation of the HCASMCs and alternative methods are required to determine the proliferation state post-stimulation.

While TLR4-mediated signalling has been implicated in the phenotypic modulation of SMCs by Sakic et al, it should be noted that it cannot be elucidated from these results whether the NF-κB activation of HCASMCs and plaque cells is mediated by TLR4. Stoll et al. have shown that when stimulating HCASMCs with low endotoxin concentrations, there was potent activation of HCASMCs as indicated by a >10 fold increase in cytokine production compared to human coronary artery endothelial cells (HCAECs).[21] Interestingly, they found that this sensitivity is not due to differential TLR4 expression, but rather due to the presence of membrane-bound CD14, which recognizes a broad range of inflammatory molecules and functions as a pattern recognition molecule.[21] Therefore, while TLR4 is present in HCASMCs, it should not be considered as the only mechanism through which NF-κB can be activated until proper experimental due diligence has been performed.[21] Thus, it cannot be unequivocally assumed that LPS-induced NF-κB activation is happening through TLR4-mediated signalling.

Sakic et al. observed a SMC phenotypic switch when stimulating the cells with S100A4, a TLR4 ligand that mediates the activation of NF-κB[11] S100A4 has both intra- and extracellular functions, where extracellular S100A4 can activate various biological processes, primarily through induction of expression of pro-inflammatory cytokines, growth factors, MMPs and stimulating of pro-inflammatory pathways.[25,26] Extracellular S100A4 can signal through either RAGE or TLR4. It was found through a

SMC TLR4-/- model that S100A4 triggers damage-associated molecular pattern (DAMP)-related pathways through its pro-inflammatory functions.[11,26] Due to these findings, we wanted to determine whether S100A4 could activate NF-κB in HCASMCs and plaque cells and whether it was capable of inducing a phenotypic switch in these cells. We found no activation of NF-κB, in both HCASMC and plaque cells, using commercially available S100A4. This was unexpected considering research found that activation of S100A4 can be induced using concentrations of 1 ug/mL, and more optimally with 2.5 ug/mL and 5.0 ug/mL.[27] Therefore, since concentrations of 2.5 ug/mL and 5.0 ug/mL both alone and in combination with PDGF-BB were used, activation of NF-κB should have been possible. It was then found that only oS100A4 in combination with PDGF-BB could induce the transition from S-SMC to R-SMC.[11] However, in the original study performed by the same group, a human recombinant, commercially purchased S100A4 protein appeared to induce the phenotypic transition, which the later research then contradicted.[11,22] However, since only 10% of SMCs in the original study demonstrated a phenotypic transition, it may be the case that S100A4 can spontaneously oligomerize, although this was not observed in this study as indicated by the lack of activation of NF-κB.[22] Therefore, it can be concluded that only oS100A4 can activate NF-κB and thereby induce phenotypic switching, and the dimeric form, and implicitly the monomeric form, cannot do the same.[11] SDS-PAGE results of the commercially purchased S100A4 confirms that the S100A4 used in this research is a monomeric form of S100A4. This therefore provides an explanation for the lack of NF-κB activation.

4. Limitations & Future Perspectives

One of the largest limitations to be addressed is the lack of quantitative methods used to assess the morphological changes and proliferation of the cells. Visual inspection is inadequate to determine whether a morphological change is occurring as the same place in the well cannot be imaged each time, and therefore the results may not necessarily be representative of all cells stimulated with that condition. One way to quantify the morphological changes observed in particularly the HCASMCs are due to phenotypic modulation, a quantitative polymerase-chain reaction (qPCR) could be used to measure the expression of SMC-specific markers such as MYOCD, SM22α and α-SMA, prior to and after stimulation. Additionally, different proliferation and apoptosis markers could also be used to assess the state of these processes, as proliferation is a known marker of R-SMCs, and potentially determine the effect of the medium composition.[11,13] Furthermore, S100A4 could be used as a marker to determine what the effect of S100A4 stimulation is on S100A4 expression in the cells, and whether this differs between the HCASMCs and plaque cells. Lastly, since Sakic et al. determined *in vivo* that stimulation of coronary arteries with S100A4 led to stabilization of the plaque, different markers associated with stable plaques could also be taken along to determine if they are upregulated when stimulating the plaque cells.

Several studies have also indicates that both LPS and S100A4 can both increase proliferation of VSMCs *in vitro* and that overexpression of NF-κB has the same effect.[15,27–29] This also indicates that proliferation may provide a quantitative method to measure the effect of S100A4 and LPS. This could be done by measuring the metabolic activity of the cells and thereby quantify cell proliferation pre- and post-stimulation. This would also provide further insight regarding the behaviour of the HCASMCs and plaque cells in response to external stimuli, regarding the plastic capabilities of the plaque cells.

Another limitation of the study is the inconsistency in the confluency of the cells at the time of stimulation. While 70-80% confluency was desired at the time of stimulation, cells in certain wells grew much quicker or much slower, meaning there was a variation of approximately 30-100% confluency between cells. There is evidence that demonstrates that phenotypic modulation can occur in response to environmental stimuli, one of which includes cell-cell interactions.[5,8,30] Therefore, it stands to reason that the cells in conditions with ~30% confluency would not respond the same as those at complete confluency. While there is no way to ensure that the same seeding density results in the same confluency, measures can be taken to ensure that confluency is roughly similar across condition, for instance by expanding to biological triplicates, instead of duplicates. Additionally, one female patient cell line was used. This sample size for both HCASMCs and plaque cells should be expanded to include more (male) patients to prove reproducibility of the results. Lastly, it should also be taken into consideration that the plaque cells may require different stimuli to the HCASMCs as they are though to exist in different states of dedifferentiation and may therefore not have the same switching capacity.

As a future perspective, to ultimately determine the capacity of S100A4 to induce phenotypic switching in HCASMCs and plaque cells, as suggested by Sakic et al., an oligomeric S100A4 (oS100A4) should be tested. To do so, at the time of writing, oS100A4 is being produced in-house for continuation of the experiments. The efficacy of this S100A4 can then be tested by i) proving NF-κB activation with the validated experimental set-up described previously and ii) determine whether phenotypic modulation of both or either HCASMCs or plaque cells can be induced. For this follow-up research, both HCASMCs and plaque cells will be used and stimulated with the in-house produced oS100A4 protein. To quantify the results, qPCR will be used to determine expression of contractile SMC markers and S100A4 to determine whether the morphological changes observed, if any, are somehow related to these markers. We will also employ metabolic assays such as PrestoBlue to enable a quantitative measure of cell proliferation, another characteristic of R-SMCs.

5. Conclusion

This research aimed to determine whether phenotypic modulation of plaque and smooth muscle cells was possible via stimulation with LPS and S100A4. It was determined that some morphological changes could be induced in the human coronary artery smooth muscle cells stimulated with LPS, although further quantification is required prior to confirmation that this is a phenotypic modulation. With S100A4 it was not possible to activate NF-κB due to its monomeric confirmation, and future research will focus on using oS100A4 to induce i) NF-κB activation and ii) phenotypic modulation of plaque cells and human coronary artery smooth muscle cells.

6. Methods

6.1. Cell Culture

6.1.1. Plaque Cell Isolation

The patient plaque to was processed immediately upon arrival from the operating room isolate Plaque cells. Under sterile conditions the direction of the plaque was identified, and the culprit lesion and the next upstream or downstream segment were cut out and processed according to relevant protocols for inclusion in the AtheroExpress biobank (link the initial paper here) and are therefore not used in PC isolation. The remaining pieces are cut into 5 mm2 pieces and washed 3x with HBSS 1x (Gibco) until the solution runs clear. Subsequently, one plaque piece per well was placed in the pre-coated 12-well plate with antibiotic medium. The pieces are left at 37°C for 3 days, after which the antibiotic medium is refreshed with freshly made antibiotic medium. This is incubated for 2 days at 37°C. From day 6 to 14, PC complete medium is used (for composition specification, see section 5.1.2) and refreshed every second day. On day 14, the pieces of plaque are removed, and medium is refreshed every 2 days until at least day 21. On day 21, the cells can be replated into a fibronectin coated T25 flask and cultured.

6.1.2. Cell Types & Media

For the initial pilot study to determine NF-κB activation, 4 different cell types were used. Medical Research Council Strain (MRC-5) fibroblasts between passage 17 and 28, human dermal microvascular endothelial cells (HMEC-1) between passage 18 and 19, human aortic smooth muscle cells (HASMC) between passage 7 and 9, human coronary artery smooth muscle cells (HCASMCs) between passage 6 and 9, and plaque inner mass cells (PC) between passage 3 and 8 were used.

For all experiments other than the initial pilot study, human coronary artery smooth muscle cells (HCASMCs) were used instead of HASMCs.

Complete Medium

The HSCASMCs and Plaque cells were cultured in the same medium. This contains 425 mL of HAMs F12K Nut Mix 1x (Gibco), 50 mL of heat inactivated fetal calf serum (HI-FCS ; Corning), 5 mL of HEPES 1M (Fisher Scientific), 5 mL of TES powder (Sigma Aldrich), 5 mL of insulin transferrin sodium selenite (ITS ; Fisger Scientific), 1 tablet of endothelial cell growth supplement (ECGS; Merck/Sigma Aldrich) dissolved in 3 mL of cold, sterile PBS (Gibco) and 5 mL of penicillin-streptomycin (P/S; Gibco). Prior to use, a 50 mL tube was supplemented with 500 uL of freshly prepared vitamin C solution (0.05g of L-ascorbic acid in 15 mL of MilliQ H_2O ; viable for 7 days after preparation). The MRC-5 fibroblasts were cultured in 450 mL of DMEM/F12 (1:1) 1x (Gibco), 45 mL of fetal bovine serum (FBS ; Corning), and 4.5 mL of P/S (Gibco). The HMECs were cultured in 450 mL of MCDB 131 Medium 1x (Gibco), 0.5 mL of hydrocortisone, 0.5 mL of human endothelial growth factor, 4.5 mL of P/S (Gibco), and 45 mL of FBS (Corning).

FCS Depletion Medium

FCS-depletion medium does not contain FCS and uses half the amount of HAMs F12K Nut Mix 1x (Gibco), and all other components present in the complete medium are doubled. Additionally, fresh vitamin C is added.

Starvation Medium

Starvation medium has the same composition as complete medium, but without FCS, ECGS, fresh Vitamin C, and ITS.

6.1.3.Cell Culture

All cell lines were initially thawed and cultured in appropriately sized cell culture flasks (BRAND), a sufficient number of cells was achieved.

Prior to plating of cells into 24-well plates (Corning), cover slips (brand) were placed at the bottom of each well used and sterilized with 70% EtOH. Each plate was then coated for the respective cell type. For HCASMCs and Plaque cells, the plates were coated with Fibronectin (VWR International) solution in PBS 1x (2 ug/cm^3). For the MRC-5 cells and HMECs, the plates were coated with 0.1% Gelatin (Gibco). Plates were then incubated for at least 30 minutes at 37 °C. Once the cells were ready to be plated, the fibronectin was removed, and medium was added to equilibrate. For the plates with a gelatin coating, the plates were washed 3x with PBS pH 7.4 1x (Gibco), and subsequently medium was added to equilibrate.

6.1.4. Plating of Cells

MRC-5s were seeded at a density of 20,000 cells per well, and the HMECs, HCASMCs, and PIs were seeded at a density of 25,000 cells per well in 24 well plates. The cells were allowed to reach approximately 80% confluency over at least 24 hours. If more time was necessary for the cells the required confluency, the medium was refreshed the day after coating and every second day thereafter. For the 8-well plates (Eppendorf) used for the S100A4 NF-κB activation, both HCASMCs and Plaque cells were seeded at a density of 10,000 cells/well.

6.1.5. Stimulation of Cells

After reaching a confluency of approximately 80%, the cells were stimulated. For the FCS-depletion and starvation conditions, cells were depleted or starved, respectively, for 24 hours prior to stimulation to ensure syncing of the cell cycle and to remove the influence of FCS and/or other growth factors and hormones.

For the pilot study NF-κB stimulation with LPS in all cell types, the cells were treated with either: i) 1 ug/mL of LPS ii) 10 ug/mL of LPS or iii) 10 ug/mL of LPS and 30 ng/mL of PDGF-BB. Cells were stimulated for 1h in complete PC medium to induce NF-κB activation and then fixed with 4% paraformaldehyde (PFA) for 15 minutes at room temperature and rinsed with PBS 1x.

For the staining optimization, only HASMCs were used and treated with either untreated or stimulated with 10 ug/mL of LPS for 1.5 hours and then fixed with 4% PFA for 15 minutes at room temperature.

For the LPS-induced phenotypic switching, complete, FCS-depletion, and starvation medium were used for both HCASMCs and Plaque cells. Prior to stimulation of cells for LPS-induced phenotypic switching, the cells in FCS-depletion and starvation medium were either depleted or starved (depending on the condition) for 24 hours prior to stimulation. Subsequently, cells were treated with either i) 10 ug/mL of LPS, ii) 10 ug/mL of LPS and 30 ng/mL of PDGF-BB, or iii) 30 ng/mL of PDGF-BB. Cells were stimulated and for 96h and medium was not changed during the time of the experiments. After 96h, the cells with fixed with 4% PFA for 15 minutes at room temperature and rinsed with PBS 1x (Gibco) three times.

HCASMCs and Plaque cells were used to induce NF-κB activation with the S100A4 protein (REF: 4137-S4, R&D Systems). Cells were stimulated with either: i) 2.5 ug/mL of S100A4, ii) 5.0 ug/mL of S100A4, iii) 2.5 ug/mL and 30 ng/mL of PDGF-BB, iv) 5.0 ug/mL and 30 ng/mL of PDGF-BB or v) 10 ug/mL of LPS and 30 ng/mL of PDGF-BB. Cells were stimulated for 1h in complete PC medium to induce NF-κB activation and then fixed with 4% paraformaldehyde (PFA) for 15 minutes at room temperature and rinsed with PBS pH 7.4 1x (Gibco).

6.2. Immunofluorescence Staining & Imaging

6.2.1. Immunofluorescent Stainings

Cells were permeabilized with 0.1% Triton X-100 in PBS 1x (Gibco) for 10 minutes, washed 3 times with PBS 1x (Gibco), and blocked with 10% normal goat serum (NGS) or 10% bovine serum albumin (BSA; BRAND) depending on the antibodies used for 1 hour. Subsequently, the slides were incubated with anti-NF-κB p65 antibody (ABCAM, CAT#ab16502) in 1% PBSA at 4°C overnight. The following day, the slides were washed 3 times with PBS 1x (Gibco) and then incubated with a secondary antibody for NF-κB and AlexaFluor labelled primary antibody for aSMA simultaneously for 1 hour. Slides were then washed with PBS 1x (Gibco) three times. Cells were then incubated in Hoechst in PBS 1x for 2 minutes and washed one time with PBS 1x (Gibco). Glass cover slips were then mounted on microscopy slides (Epredia, REF#J1800AMNZ) using Fluoromount-G® (SouthernBiotech; CAT#0100-01) and stored at 4°C for short-term storage and -20°C for long-term storage.

Different secondary antibodies were used for NF-κB staining and primary aSMA staining, as noted in Tables XX and XX. All experiments other than the pilot NF-κB activation stainings were blocked with 10% BSA (brand). The dilution used for each experiment can be found in Table XX and further information on the primary and secondary antibodies used can be found in Table XX and Table XX, respectively.

Table 1. Antibody dilutions used for each experiment.

Experiment	Staining specific for	Dilution
Pilot NF-κB Activation	NF-κB	1:500
Pilot NF-κB Activation	ASMA	1:500
All Experiments	Nuclei	1:10000
Staining Optimization	NF-κB	1:1500
Staining Optimization	NF-κB	1:2000
Staining Optimization	ASMA	1:100
Staining Optimization	ASMA	1:150
LPS-induced Phenotypic Switching & S100A4 NF-κB Activation	NF-κB	1:1500
LPS-induced Phenotypic Switching & S100A4 NF-κB Activation	AMSA	1:200

Table 2. List of primary antibodies used. Includes in which experiment the antibody was used and relevant information about the antibody.

Antibody specific for & label	Experiment	Clone	Class/Host/Isotope	Provider
Alpha-SMA (AlexaFluor 488)	Pilot NF-κB Activation	1A4	Monoclonal/Mouse /IgG2a	Invitrogen (REF#53-9760-82)
Alpha-SMA (AlexaFluor 594)	Staining Optimization	1A4	Monoclonal/Mouse/IgG2a	ABCAM (CAT#ab202368)
NF-κB p65 (unlabelled)	Pilot NF-κB Activation		Polyclonal/Rabbit/IgG	ABCAM (CAT#ab16502)
Nuclei	All Experiments	N/A	N/A	Thermofisher Scientific(Hoechst

33342,
CAT#H1399)

Table 3. List of Secondary antibodies. Includes in which experiment the antibody was used and relevant information about the antibody.

Secondary antibody targeting & label	Experiment	Clone	Species Reactivity/Class/Host/Isotope	Provider
NF-κB p65 (AlexaFluor 555)	Pilot NF-κB Activation		Rabbit/Polyclonal/Goat/IgG	Invitrogen (REF#A2148)
NF-κB p65 (AlexaFluor 488)	Staining Optimization		Rabbit/Polycloncal/Goat/IgG	Invitrogen

6.2.2.Imaging

For imaging of the slides, the Olympus BX53 microscope was used with Cellsens software. All images for the pilot NF-κB activation using LPS and staining optimization were taken at 10x magnification, whereas the images for the NF-κB activation experiment using S100A4 were taken at 20x magnification. For the transmitted light images, an EVOS FLoid imaging system was used (REF# 4471136)

6.3. SDS-PAGE

To determine the conformation of the S100A4 protein (REF: 4137-S4, R&D Systems), an SDS-PAGE was performed. Sample buffer containing Tris , SDS, Glycerol, trypan blue and MilliQ water was used. The PageRuler™ Plus Prestained Protein ladder (REF#26619) was used as a protein ladder. Subsequently,10 ul of the S100A4 protein was unfolded at 95°C for 5 minutes and subsequently loaded in an in-house made polyacrylamide gel at 170V for 1 hour and subsequently stained with SimplyBlue™ SafeStain (Invitrogen, CAT#LC6060) as per the manufacturers instructions.

References

1. Libby, P. *et al.* Atherosclerosis. *Nat. Rev. Dis. Prim.* **5**, 56 (2019).
2. Libby, P., Ridker, P. M. & Hansson, G. K. Progress and challenges in translating the biology of atherosclerosis. *Nature* **473**, 317–325 (2011).
3. Zhu, Y. *et al.* Research Progress on the Relationship between Atherosclerosis and Inflammation. *Biomolecules* **8**, (2018).
4. Bennett, M. R., Sinha, S. & Owens, G. K. Vascular Smooth Muscle Cells in Atherosclerosis. *Circ. Res.* **118**, 692–702 (2016).
5. Zhang, F., Guo, X., Xia, Y. & Mao, L. An update on the phenotypic switching of vascular smooth muscle cells in the pathogenesis of atherosclerosis. *Cell. Mol. Life Sci.* **79**, 6 (2021).
6. Buono, M. F. *et al.* The changing landscape of the vulnerable plaque: a call for fine-tuning of preclinical models. *Vascul. Pharmacol.* **141**, 106924 (2021).
7. Grootaert, M. O. J. & Bennett, M. R. Vascular smooth muscle cells in atherosclerosis: Time for a re-assessment. *Cardiovascular Research* vol. 117 (2021).
8. Chakraborty, R. *et al.* Targeting smooth muscle cell phenotypic switching in vascular disease. *JVS-Vascular Sci.* **2**, 79–94 (2021).
9. Basatemur, G. L., Jørgensen, H. F., Clarke, M. C. H., Bennett, M. R. & Mallat, Z. Vascular smooth muscle cells in atherosclerosis. *Nat. Rev. Cardiol.* **16**, 727–744 (2019).
10. Zheng, B., Han, M. & Wen, J.-K. Role of Krüppel-like factor 4 in phenotypic switching and proliferation of vascular smooth muscle cells. *IUBMB Life* **62**, 132–139 (2010).
11. Sakic, A. *et al.* Neutralization of S100A4 induces stabilization of atherosclerotic plaques: role of smooth muscle cells. *Cardiovasc. Res.* **118**, 141–155 (2022).
12. Hao, H. *et al.* Heterogeneity of Smooth Muscle Cell Populations Cultured From Pig Coronary Artery. *Arterioscler. Thromb. Vasc. Biol.* **22**, 1093–1099 (2002).
13. Brisset, A. C. *et al.* Intimal smooth muscle cells of porcine and human coronary artery express S100A4, a marker of the rhomboid phenotype in vitro. *Circ. Res.* **100**, 1055–1062 (2007).
14. Newman, A. A. C. *et al.* Multiple cell types contribute to the atherosclerotic lesion fibrous cap by PDGFRβ and bioenergetic mechanisms. *Nat. Metab.* **3**, 166–181 (2021).
15. Yin, Q. *et al.* LPS Promotes Vascular Smooth Muscle Cells Proliferation Through the TLR4/Rac1/Akt Signalling Pathway. *Cell. Physiol. Biochem. Int. J. Exp. Cell. Physiol. Biochem. Pharmacol.* **44**, 2189–2200 (2017).
16. Jiang, D., Yang, Y. & Li, D. Lipopolysaccharide induced vascular smooth muscle cells proliferation: A new potential therapeutic target for proliferative vascular diseases. *Cell Prolif.* **50**, e12332 (2017).
17. Zhang, X. *et al.* Interleukin-1/Toll-Like Receptor-Induced Nuclear Factor Kappa B Signaling Participates in Intima Hyperplasia after Carotid Artery Balloon Injury in Goto-Kakizaki Rats: A Potential Target Therapy Pathway. *PLoS One* **9**, e103794 (2014).
18. Moriyama, K. & Nishida, O. Targeting Cytokines, Pathogen-Associated Molecular Patterns, and Damage-Associated Molecular Patterns in Sepsis via Blood Purification. *International Journal of Molecular Sciences* vol. 22 (2021).
19. Jiang, D. *et al.* Positive Feedback Regulation of Proliferation in Vascular Smooth Muscle Cells Stimulated by Lipopolysaccharide Is Mediated through the TLR 4/Rac1/Akt Pathway. *PLoS One* **9**, e92398 (2014).
20. Ernst, O., Vayttaden, S. J. & Fraser, I. D. C. Measurement of NF-κB Activation in TLR-Activated Macrophages. *Methods Mol. Biol.* **1714**, 67–78 (2018).
21. Stoll, L. L. *et al.* Regulation of endotoxin-induced proinflammatory activation in human coronary artery cells: expression of functional membrane-bound CD14 by human coronary artery smooth muscle cells. *J. Immunol.* **173**, 1336–1343 (2004).
22. Chaabane, C., Heizmann, C. W. & Bochaton-Piallat, M.-L. Extracellular S100A4 induces smooth muscle cell phenotypic transition mediated by RAGE. *Biochim. Biophys. Acta - Mol. Cell Res.* **1853**, 2144–2157 (2015).
23. Strela, F. B. *et al.* Lipopolysaccharide exposure modulates the contractile and migratory phenotypes of vascular smooth muscle cells. *Life Sci.* **241**, 117098 (2020).
24. Xia, C., Braunstein, Z., Toomey, A. C., Zhong, J. & Rao, X. S100 Proteins As an Important

Regulator of Macrophage Inflammation. *Front. Immunol.* **8**, 1908 (2017).
25. Garrett, S. C., Varney, K. M., Weber, D. J. & Bresnick, A. R. S100A4, a mediator of metastasis. *J. Biol. Chem.* **281**, 677–680 (2006).
26. Li, Z., Li, Y., Liu, S. & Qin, Z. Extracellular S100A4 as a key player in fibrotic diseases. *J. Cell. Mol. Med.* **24**, 5973–5983 (2020).
27. Cardoso Dos Santos, L. M., Ambartsumian, N., Grigorian, M. & Bochaton-Piallat, M. L. Role of S100A4 in atherosclerosis development. *Eur. Heart J.* **42**, ehab724.3399 (2021).
28. Nagata, M. *et al.* Calcium-Binding Protein S100A4 Is Upregulated in Carotid Atherosclerotic Plaques and Contributes to Expansive Remodeling. *J. Am. Heart Assoc.* **9**, e016128 (2020).
29. Jiao, L., Jiang, M., Liu, J., Wei, L. & Wu, M. Nuclear factor-kappa B activation inhibits proliferation and promotes apoptosis of vascular smooth muscle cells. *Vascular* **26**, 634–640 (2018).
30. Owens, G. K., Kumar, M. S. & Wamhoff, B. R. Molecular Regulation of Vascular Smooth Muscle Cell Differentiation in Development and Disease. *Physiol. Rev.* **84**, 767–801 (2004).

Supplementary Figures

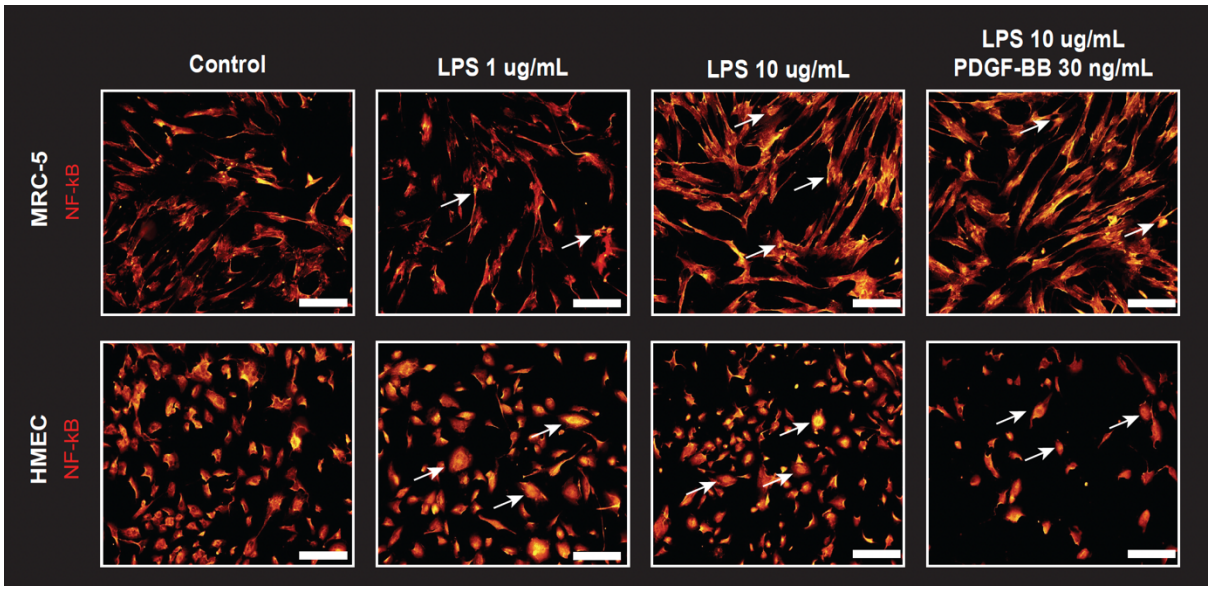

Figure S1. LPS-induced NF-κB activation in MRC-5s and HMECs. MRC-5s and HEMCs stimulated with i) LPS at 1 ug/mL ii) LPS at 10 ug/mL or iii) LPS at 10 ug/mL PDGF-BB. Activation of the NF-κB pathway is shown by illuminated nuclei. Abbreviations: HASMC: human aortic smooth muscle cells; PC: plaque cells ; LPS : Lipopolysaccharide ; PDGF-BB : platelet-derived growth factor BB; NF-κB : Nuclear transcription factor kappa B.

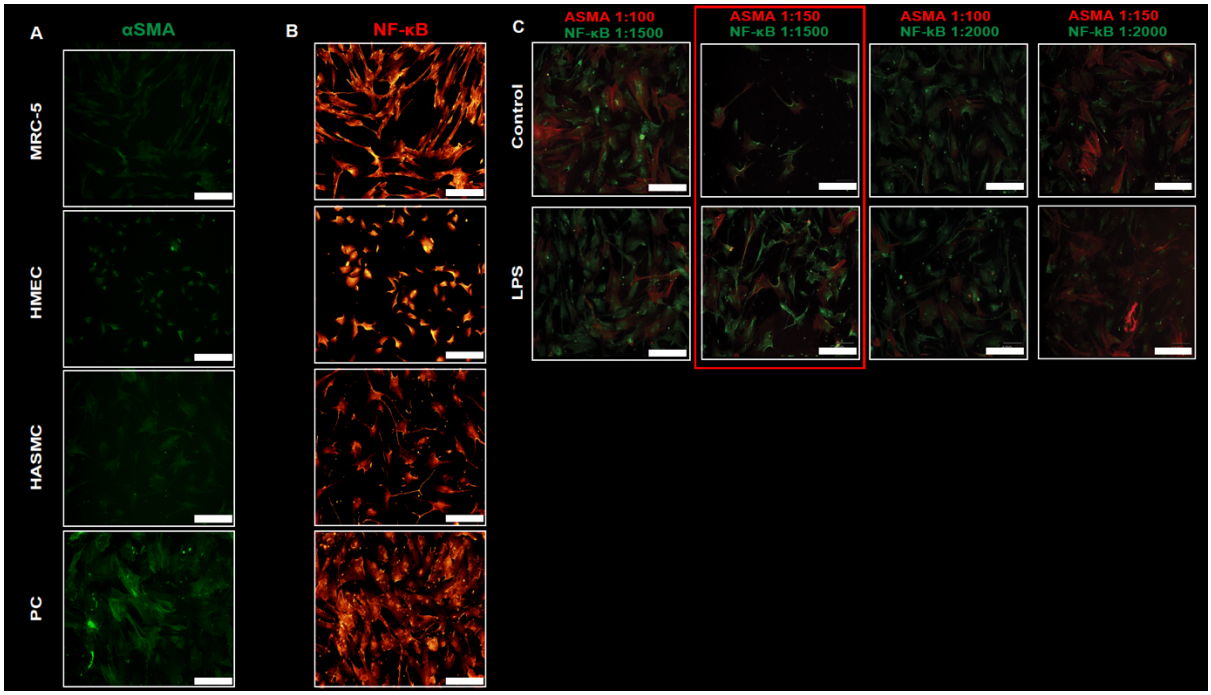

Figure S2. Staining Optimization for αSMA and NF-κB performed on HASMCs. A. Initial dilution (1:500) used to stain for αSMA. Scale bar is 100 µm, images taken at 10x magnification. B. Initial dilution (1:500 for primary antibody, 1:400 for secondary antibody) used to stain for NF-κB activation. Scale bar is 100 µm, images taken at 10x magnification. C. Different combinations of primary antibody dilutions used for both NF-κB activation and αSMA. The optimal combination of dilutions (1:150 for αSMA and 1:1500 for NF-κB activation) is marked with the red box. Scale bar is 100 µm, images taken at 10x magnification. Abbreviations: α-SMA: alpha smooth muscle actin.; NF-κB: Nuclear transcription factor kappa B; LPS: lipopolysaccharide

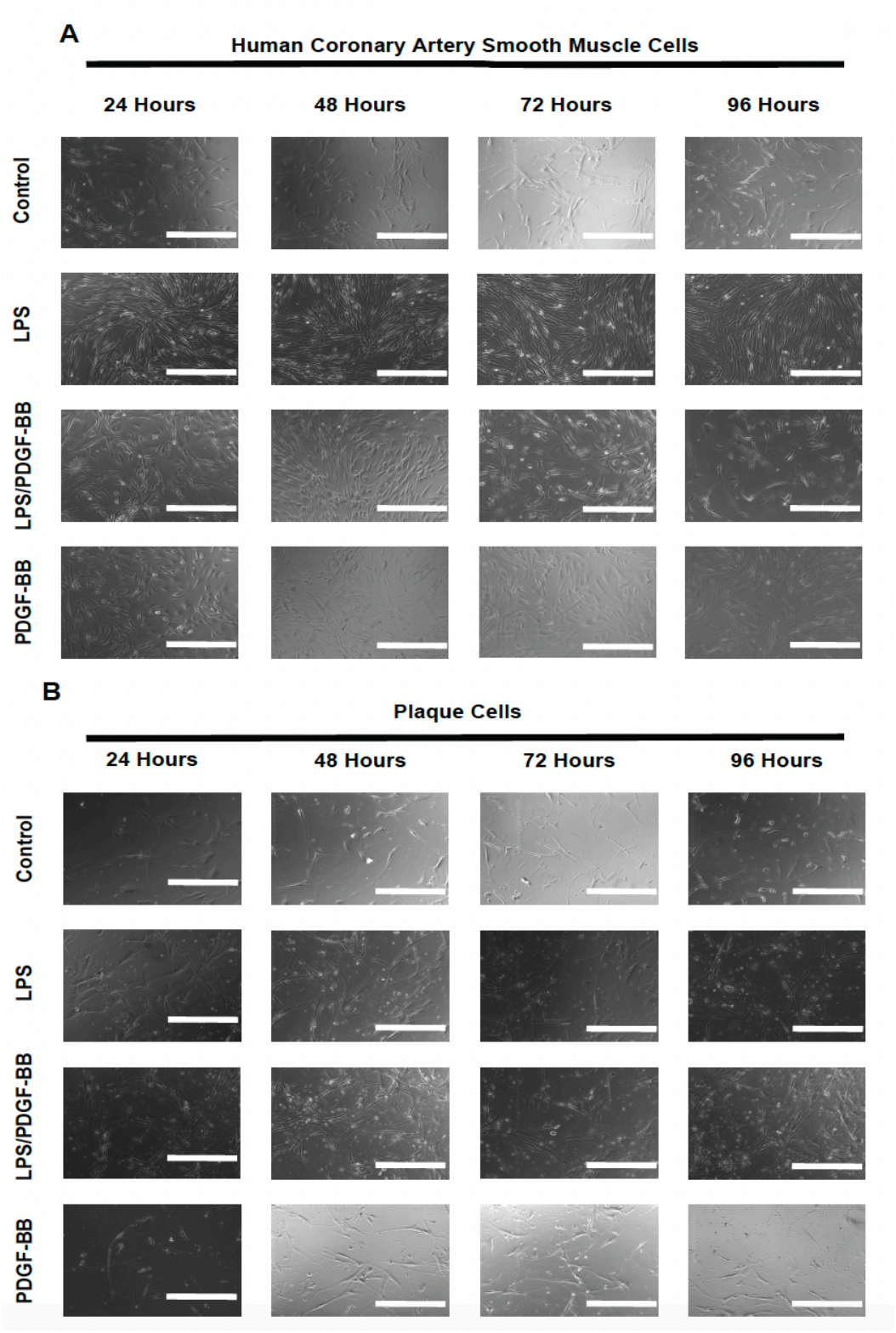

Figure S3. Morphological Changes in Human coronary artery smooth muscle cells and plaque cells cultured in starvation medium taken at 10x magnification. A. Process of morphological changes starting 24 hours post-stimulation of the human coronary artery smooth muscle cells. B. Process of morphological changes starting 24 hours post-stimulation of the plaque cells. Scale bar: 400 µm. Abbreviations: LPS: Lipopolysaccharide; PDGF-BB: platelet-derived growth factor BB; H: hours

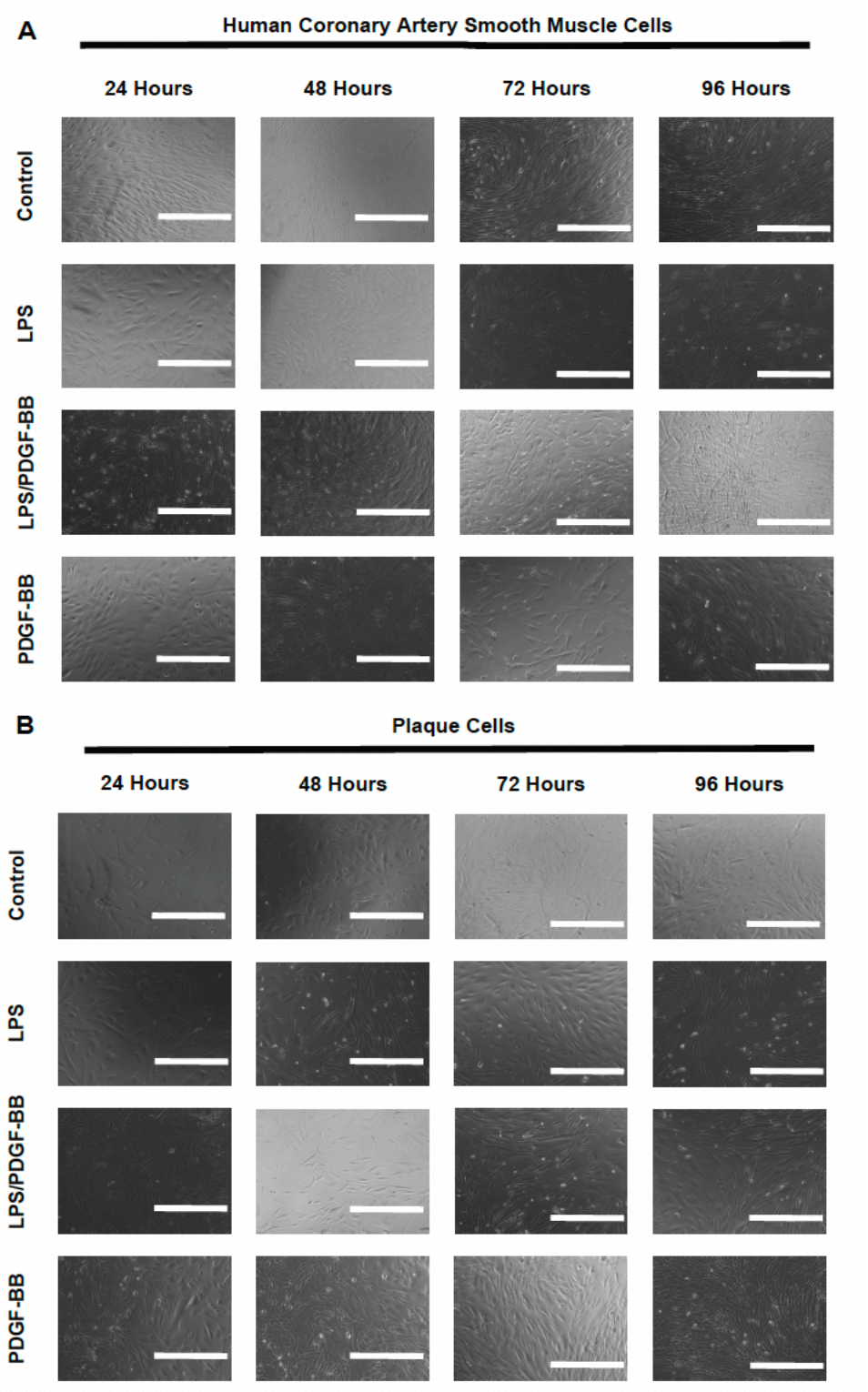

Figure S4. Morphological Changes in Human coronary artery smooth muscle cells and plaque cells cultured in complete medium taken at 10x magnification. A. Process of morphological changes starting 24 hours post-stimulation of the human coronary artery smooth muscle cells. B. Process of morphological changes starting 24 hours post-stimulation of the plaque cells. Scale bar: 400 µm. Abbreviations: LPS: Lipopolysaccharide; PDGF-BB :platelet-derived growth factor BB; H: hours

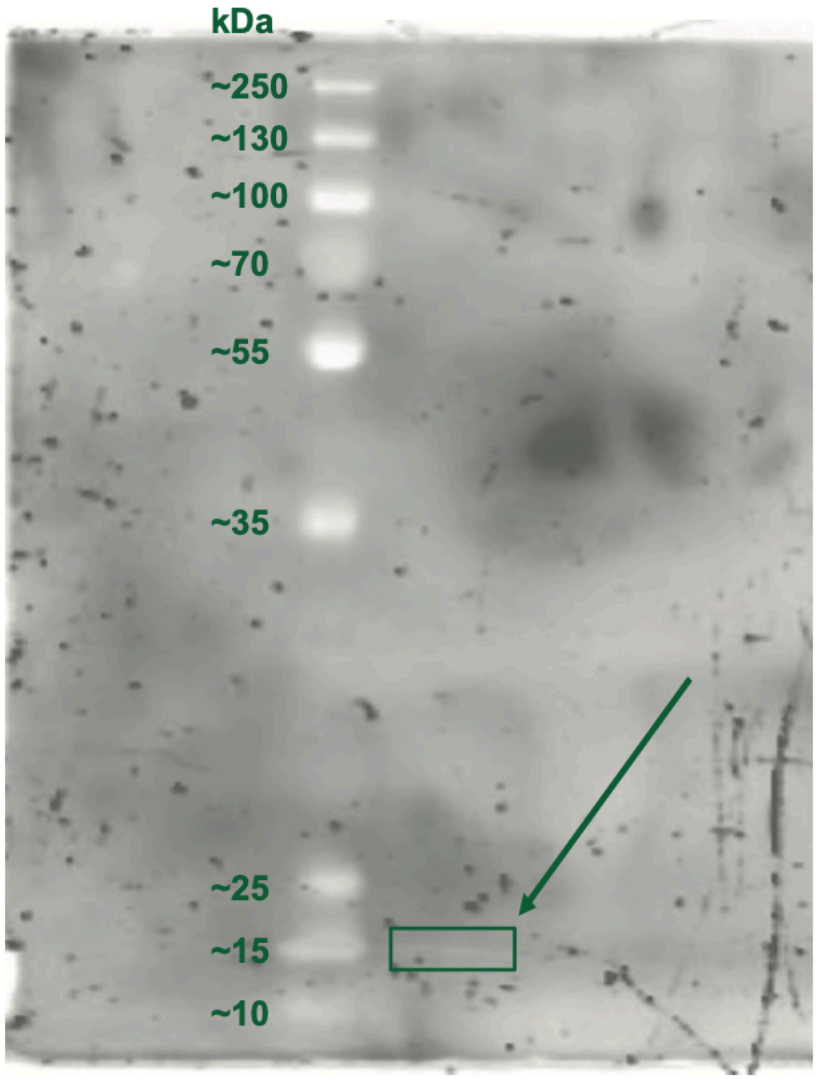

Figure S5. SDS-PAGE results for the human recombinant S100A4 protein. Demonstrates that the S100A4 used in this research is of a monomeric conformation, as indicated by the band at 15 kDa, indicated by the green arrow. Abbreviations: kDA: kilodaltons